Egyptian Journal of Geology

https://egjg.journals.ekb.eg

An integrated assessment of the groundwater chemistry of the aquifers at North Giza Governorate, using multivariate statistical analysis, ionic ratios, and geochemical modeling

Shereen A. Nasr [1], Ali Abdel-Motelib Ali[1], Taher M. H.[2], and **Hend S. Abu Salem[1]**

[1]*Geology Department, Faculty of Science, Cairo University, Egypt*
[2]*Central Laboratory for Environmental Quality Monitoring, National Water Research Centre, El-Qanater El-Khairia, Egypt*

GROUNDWATER is an important source of water in Egypt that has been heavily exploited in recent decades. This has led to the expansion of the west Nile Delta cultivated area through the New Delta project (in the area to the west of the old Nile Delta), that pose additional stresses on the water resources. Fourteen groundwater samples from the semi-confined and five samples from the unconfined Quaternary aquifers were collected, thirteen samples from the Miocene (Moghra) aquifer, and one sample from the deep Nubian aquifer were also collected and analyzed for various parameters. A comprehensive assessment of the four aquifers in the study area were done using statistical analysis, biplots, Piper and Gibb's diagrams, as well as temporal comparison of the water chemistry. The statistical analysis output indicates the interplay between human activities (anthropogenic factors) and the interaction with the bearing rocks (geogenic factors) that affect the water chemistry of the aquifers. The hydrogeochemistry of the different aquifers indicates that the semi–confined Quaternary and the Moghra aquifers are best used for irrigation, while the unconfined Quaternary aquifer belongs to the Na-Cl water type and the deep Nubian aquifer water is brine according to the salinity classification. Additionally, caution must be taken to mitigate the potential impact of contamination from the use of fertilizers and excessive pumping on the groundwater quality.

Keywords: Hydrogeochemical processes, Water quality, Moghra Aquifer, Quaternary Aquifer, Nubian Aquifer, Abu Roash, Egypt.

1. Introduction

Egypt is considered one of the driest countries in the world, where precipitation is limited, and the Nile River is the main source of fresh surface water (Mohammed et al., 2016). In recent years, the increase in water demands due to increased developmental activities and population bear stresses to the Egyptian water resources. Additionally, water shortage and scarcity as a consequence of the possible decrease of the River Nile share are expected (Abdelhafez et al., 2020). Therefore, groundwater play an important role in providing water for various purposes and sustaining life across the country. Not only groundwater is an essential source of drinking water, but it is also vital for irrigation and agricultural activities, industrial processes, and domestic uses (Dawoud et al., 2005). Agricultural activities account for the majority of Egypt's water consumption, accounting for about 85% of the country's water use (Abdin & Gaafar, 2009). Groundwater plays a significant role in irrigating agricultural lands, especially in areas where surface water is insufficient. In Egypt, the agricultural sector depends heavily on groundwater, which is withdrawn from various aquifers across the

*Corresponding author e-mail:geo.shereen@yahoo.com
Received: 29/05/2023; Accepted: 13/08/2023
DOI: 10.21608/EGJG.2023.214128.1049
©2023 National Information and Documentation Center (NIDOC)

country, including the Nubian aquifer, the Moghra aquifer, and the Quaternary aquifer (El-Rawy et al., 2020). To ensure the sustainable use of this resource, it is essential to understand groundwater chemistry and the proceeding chemical changes it encounters with time (Li et al., 2017). In this context, this research aims to conduct an integrated assessment of the groundwater chemistry of the aquifers to the west Nile Delta.

The west Nile delta area is one of the Egyptian regions that is mainly depends on the groundwater from different aquifers including the Quaternary, the Moghra aquifer, and the Pliocene aquifer (Sharaky et al., 2007). So, this work focuses on the groundwater chemistry of the aquifers in Abu Roash area namely; the unconfined and semi-confined Quaternary aquifer, the Miocene aquifer, and the deep Nubian aquifer. Accordingly, fourteen groundwater samples were collected from the semi-confined Quaternary aquifer, thirteen samples from the Miocene aquifer during the summer of 2021. Additionally, five groundwater samples were collected from the unconfined Quaternary aquifer, and one sample from the deep Nubian aquifer during the summer of 2018 from a deep well aiming to study the chemical characteristics of the groundwater and the possible changes in groundwater quality due to expanded exploitation.

The integration of hydrochemical studies with statistical analysis is imperative to understand processes that govern the chemical composition of water (El Alfy et al., 2017). In recent years, the use of modeling techniques has become popular to unravel the complex interplay of hydrological, geological, and geochemical processes that affect water quality (Mfonka et al., 2021; Mohammed et al., 2022). At the west delta area, the application of such techniques has been highly beneficial to study the hydrochemical characteristics of the groundwater system and to identify key factors that control water chemistry. One of the major hydrochemical models used for water analysis is the Gibbs diagram. The Gibbs diagram is a graphical representation of the chemical composition of water in terms of its major ions, temperature, and pH. This model is highly useful in analyzing the geochemical processes that are responsible for controlling the water chemistry in a particular region (Kumar et al., 2012). In the case of the west delta area, the Gibbs diagram has been extensively used to study the sources of dissolved ions in groundwater and to identify the dominant geochemical processes that influence water chemistry (Salem & Osman, 2017). Another hydrochemical model that has been widely used for studying water quality is the Piper diagram. This diagram is a graphical representation of the water chemistry in terms of its major cations and anions where it helps to identify the dominant chemical facies and the ions' relative proportions in the water (Piper, 1944). Integration of hydrochemical models such as Gibbs diagram and Piper diagram with statistical analysis techniques such as Pearson correlation, factor analysis, and hierarchical cluster analysis has been highly useful in understanding the complex interplay of hydrological, geological, and geochemical processes that impact the water quality.

Pearson correlation analysis helps to identify the linear relationships between different chemical parameters and to evaluate their relative importance in controlling water chemistry. Factor analysis helps to identify the dominant factors that control water chemistry, while cluster analysis is used to classify water samples into groups based on their chemical properties (Garizi et al., 2011). Finally, the findings of this research can aid in the development and management of groundwater in the study area.

2. Study area

The study area is characterized by an arid climate that is typified by hot humid summer and cold dry winter. The temperature generally ranges from 10 to 35°C throughout the year, with temperatures seldom falling below 7°C or rising over 39°C (El-Rawy et al., 2020).

The study area is characterized by two main geomorphic units; the young alluvial plain and the old alluvial plain (Shata & El Fayoumi, 1967). It expands from west Giza to the east of Cairo-Alexandria desert road about 55 km wide in the northeast of the Egyptian Western Desert. It lies between latitudes 30º 02' ·0" and 30º 17' 00" N, and longitudes 30º 40' 00" and 31º 12' 00" E including many agricultural lands (Fig. 1).

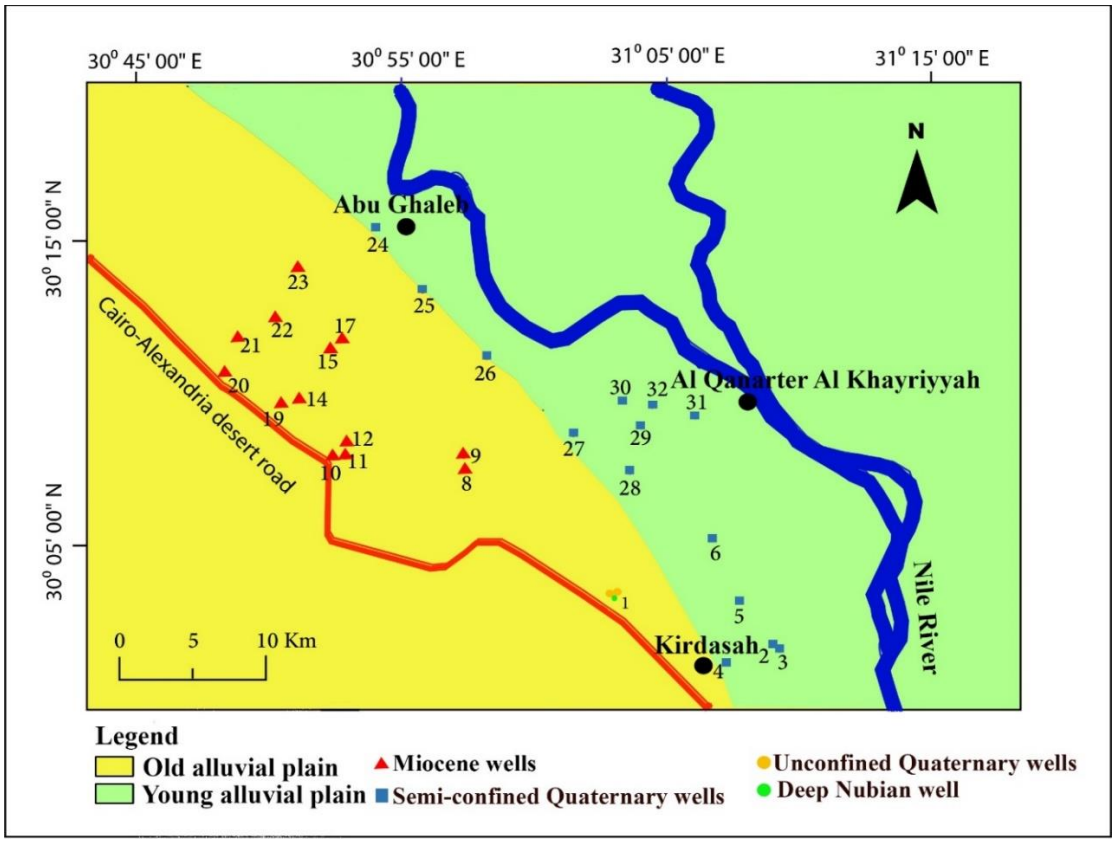

Fig. 1. Base map showing the location of the groundwater samples.

2.1 Geomorphology

The topography of Abu Roash area is mostly controlled by its structure, which consists of a hilly area controlled by several folds that are dismembered by various types of faults (Khalek et al., 1989) The surface is covered by the Upper Cretaceous chalky white limestone (Abu Roash Formation) and the Oligocene to the Lower Miocene sand and gravel that is overlying the Eocene limestones (El-Etr & El-Baz, 1979). Shata and El Fayoumy (1967) divided the west of Cairo area into four geomorphic units; namely: the alluvial plains, the structural plains, the tablelands, and the drifting sand. The alluvial plain is divided into the young and old alluvial plains which are the most outstanding geomorphic features in the west Nile Delta with elevations ranging from 0 to 20 meters above sea level with some structural hills like Gebel Abu Roash and Gebel El Mansouria (Mohallel, 2020). The study area is sloping toward the east with elevations changing from less than 50 m a.s.l. at the east to more than 150 m a.s.l. at the west of the area of consideration (Ibrahem, 2020).

2.2. Geological and Hydrogeological setting

Because of the unique exposure of the Cretaceous rocks at Abu Roash area as a consequence of a series of folding and faulting, it attracted a lot of geological attention. A deep well drilled at Abu Roash area demonstrated a complete subsurface section started from the bottom with the Carboniferous sand over the basement at depth 1901 m followed by the Jurassic

intercalations of sand, shale, and limestone then a Lower Cretaceous sand, all composed the Nubian Sandstone Formation, and finally a Cenomanian limestone and shale intercalations covered by the Pliocene sand and shale (Said, 1962) (Fig. 2).

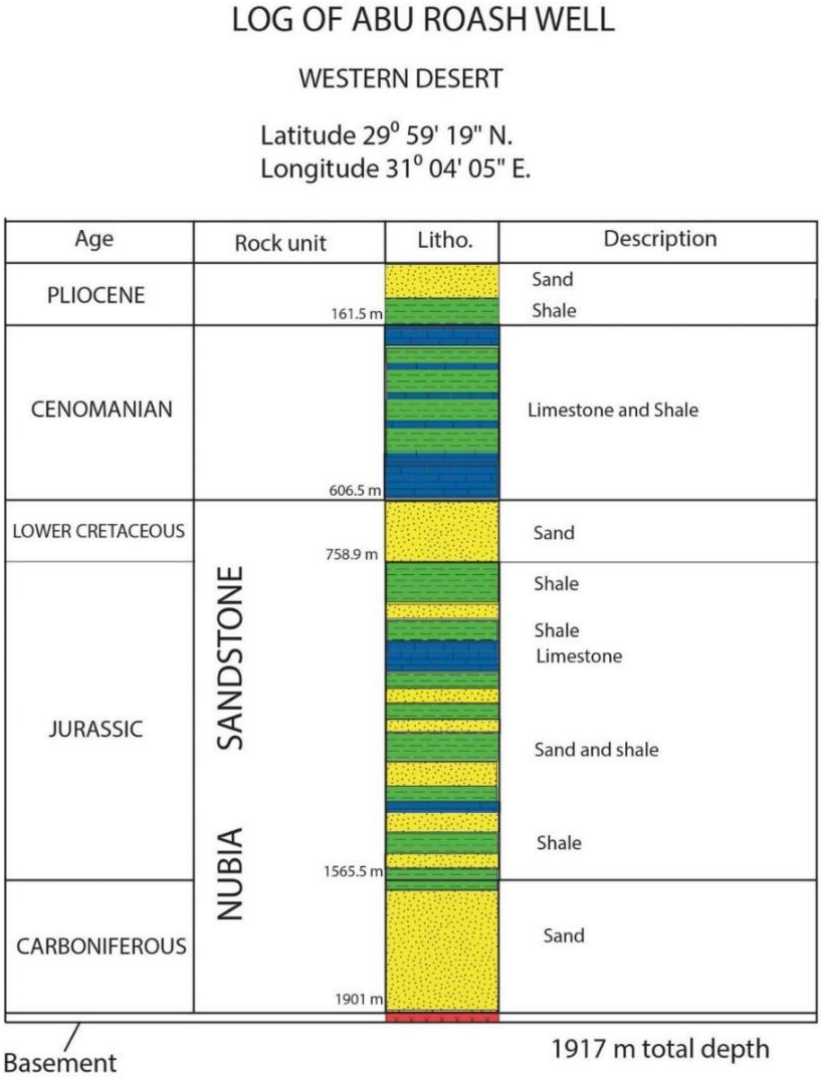

Fig. 2. Subsurface stratigraphic section at Abu Roash area (modified after Said, 1962).

The Delta Basin is separated from the land to the west by a large fault that runs roughly parallel to the Rosetta branch in NW-SE direction. The dissecting faults and uplifting resulted in a full section of the Upper Cretaceous rocks in Abu Roash area (part of the Syrian Arc Fold Belt) (Abdel-Gawad et al., 2011). According to Sehim (1986), Abu Roash district is sited on the Kattanyia Horst in the northwestern desert and was affected by many surface and subsurface structures.

From the hydrogeological standpoint, the west of the Nile Delta region contains three semi-confined aquifers; the Quaternary, the Pliocene, and the Lower Miocene aquifers. The Quaternary aquifer (the semiconfined and the unconfined) is located in the north of the Western Desert and consists of two

layers; the upper layer is composed of Holocene deposits, while the lower layer is formed of Pleistocene and Pliocene sediments (El Tahlawi et al., 2008). This aquifer is composed of unconfined portion consisting mainly of sand, where the semi-confined portion consists of graded sand and gravel intercalated with clay lenses (Omar, 2021) The rainfall represents the main recharge to the Quaternary aquifer in addition to minor contribution from the Nile River (El-Rawy et al., 2020). The Quaternary aquifer thickness varies from 20 to 140m with a groundwater flow towards the northwest (Emara et al., 2007) (Fig. 3a), The groundwater in this aquifer is generally of good quality and is suitable for irrigation purposes (Masoud, 2014).

The Lower Miocene aquifer is represented by the Moghra aquifer that lies to the west of the study area and is composed of gravel and sand with a thickness variation from 50 to 250m (El-Fakharany, 2013). The groundwater flows toward the Qattara depression by a hydraulic gradient doesn't exceeding 0.2 m/km (Eltarabily & Moghazy, 2021) (Fig. 3b) while the recharge is from the Nile River. The groundwater quality is generally good (Dawoud et al., 2005).

The Nubian Aquifer stretches all the way to Aswan from north to south. One kilometer depth of highly salinized groundwater has been discovered west of Cairo (El Tahlawi et al., 2008).

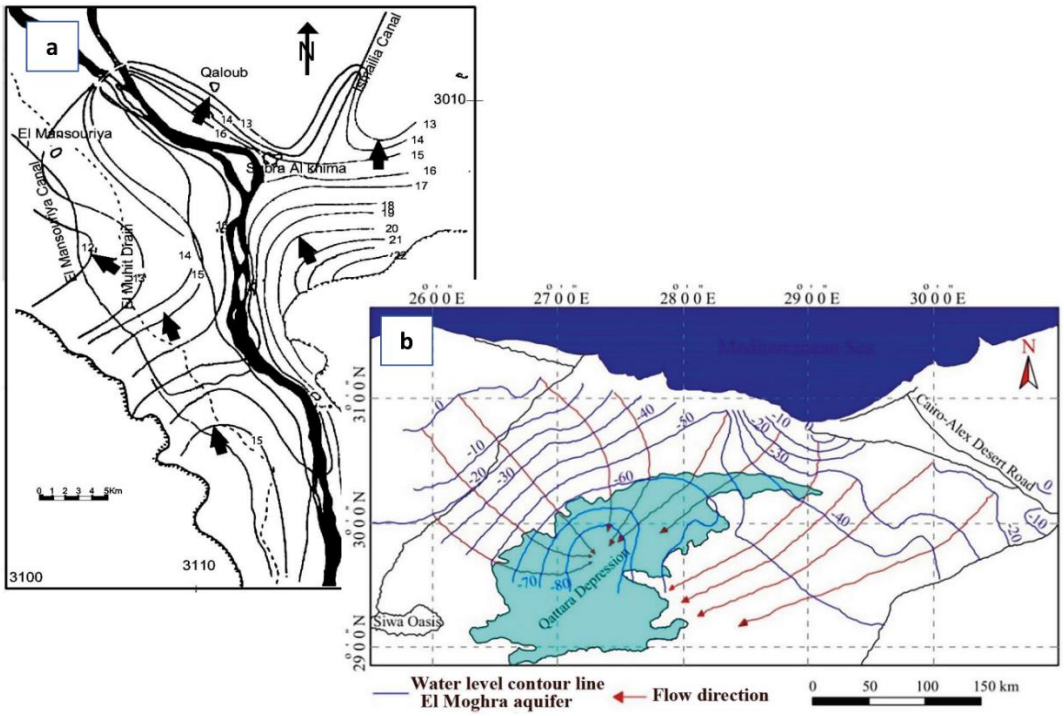

Fig. 3. Groundwater flow map, a) for the Quaternary aquifer (Emara et al., 2007) and b) for the Miocene (Eltarabily & Moghazy, 2021).

3. Methodology

Groundwater samples were collected in duplicates to be analyzed after sufficient drainage from wells as the following: The temperature, electrical conductivity, total dissolved solids, and pH of the groundwater samples were measured in situ using pH meter (YSI Model 63). Major cations (K^+, Na^+, Mg^{2+}, and Ca^{2+}) and heavy metals (Al, As, Ba, Cd, Co, Cr, Cu, Fe, Mn, Ni, Pb, Sb, Se, Sn, V, Zn) were analyzed at the National Water Research Centre (NWRC) by

Inductively Coupled Plasma-Emission Spectrometry (ICP-ES) with ultra-sonic Nebulizer USA (model Perkin Elmer Optima 3000, USA) (Table S1). Additionally, the major anions were measured at the National Water Research Centre (NWRC) using ion chromatography (IC- model DX-600, USA) instrument (Table S1), while the TDS was obtained by gravitational method (Table S1). Accordingly, fourteen groundwater samples were collected from the semi-confined Quaternary aquifer, and thirteen samples from the Miocene aquifer during the summer of 2021 (Table S1). Additionally, five groundwater samples were collected from the unconfined Quaternary aquifer and one sample from the deep Nubian aquifer during the summer of 2018 (Table S1) aiming to study the chemical characteristics of the groundwater and the possible changes in groundwater quality due to expanded exploitation. IBM® SPSS® Statistics (Version 22) software was used for the statistical analysis of the analyzed samples (e.g., descriptive statistics, Pearson correlation, factor analysis, and Hierarchical cluster analysis).

Aquachem Version 2014.2 was applied for drawing Stiff diagrams while RockWorks15 software was used for drawing Piper diagram to determine the hydrogeochemical facies and processes with the aid of Gibb's diagram and ionic ratios. The saturation indices and ion activities were calculated using PHREEQC interactive 3.4.0-12927 code. In addition, the chemical analysis from a previous work for the semi-confined Quaternary aquifer and the Moghra aquifer in 2018 (Mohallel, 2020) (Table S4) was compared with the recent analysis (2021) using box and whisker plots to investigate the temporal changes in water quality.

4. Results and discussion

4.1. Physicochemical parameters

The descriptive statistics of the analyzed data representing the semi-confined and the unconfined Quaternary aquifers, and the Miocene aquifer (Moghra aquifer) were calculated, and the maxima were compared with the Environmental Protection Agency (Environmental Protection Agency of Water, 2018), World Health Organization (WHO, 2011), and the Egyptian Health Authority (Egyptian Health Authority, 2007) (Tables 1, 2, and 3). The pH values of the semi-confined and the unconfined Quaternary, and the Moghra aquifers vary from 7.66 to 8.18, 7.89 to 8.23, and 7.38 to 8.23, respectively, which shows normal ranges for drinking water according to drinking water standards, while the salinity values of the semi-confined Quaternary, unconfined Quaternary, and the Moghra aquifers vary from 321 to 1975 ppm, 7678 to 8342 ppm, and 357 to 2250 ppm, respectively (Tables 1, 2, and 3). According to the water salinity classification of Mayer (Mayer et al., 2005) (Table 4), the semi-confined Quaternary aquifers water quality varies from freshwater that can be used for drinking and irrigation to brackish water that can be used in irrigation with caution. The Moghra aquifer water quality ranges from freshwater to moderately saline which belongs to primary drainage. Additionally, the unconfined aquifer shows saline water quality. The deep Nubian aquifer water sample analysis shows a very high salinity (86940 ppm) (Table S1) indicating that the water is brine according to the Mayer salinity classification (Mayer et al., 2005) (Table 4). According to the guidelines for water quality of drinking water (Egyptian Health Authority, 2007; Environmental Protection Agency of Water, 2018; WHO, 2011), the pH value (7.95) of the deep Nubian aquifer water sample lies in the normal drinking water range, while the salinity increases by 86.9 folds than the normal drinking range.

Table 1. Descriptive statistics of the analyzed semi-confined Quaternary groundwater samples. Concentrations and TDS are in ppm, temperature is in °C, and EC is in mmhos/cm,. Guidelines for water quality of drinking water (Egyptian Health Authority, 2007; Environmental Protection Agency of Water, 2018; WHO, 2011).

Parameters	Min.	Max.	Mean	S.D.	EPA, 2018	WHO, 2011	EHA, 2007
TDS	321.00	1975.00	757.50	447.70	500	1000	1000
pH	7.66	8.18	7.88	0.16	6.5-8.5	6.5-8.5	6.5-8.5
EC	0.50	3.09	1.18	0.70	--	--	--
Ca^{2+}	41.00	230.00	88.10	50.40	--	--	--
K^{+}	5.00	16.00	7.93	2.67	--	--	--
Mg^{2+}	17.00	69.98	32.30	13.97	--	--	--
Na^{+}	30.00	300.00	98.29	77.05	200	200*	200
HCO_3^{-}	175.00	340.00	253.71	51.83	--	--	--
F^{-}	0.07	0.73	0.21	0.16	2	1.5	2
Cl^{-}	25.86	575.00	128.35	148.37	250	250*	250
NO_3^{2-}	0.10	57.29	9.02	17.63	10	50	45
SO_4^{2-}	23.73	375.00	146.43	105.84	250	500**	250
Ba	0.07	0.24	0.15	0.05	2	0.7	0.7
Cr	0.01	0.07	0.02	0.02	0.1	0.05	0.05
Co	0.00	0.01	0.01	0.01	--	--	--
Cu	0.00	0.02	0.01	0.01	1.3	2	2
Fe	0.01	0.46	0.23	0.15	0.3	0.3	0.3
Mn	0.06	2.61	1.06	0.74	0.05	0.4	0.4
Ni	0.00	0.01	0.01	0.01	0.02	0.07	0.02
V	0.00	0.04	0.01	0.01	--	--	--
Zn	0.01	0.14	0.03	0.03	5	3	3

*Taste threshold only, no health-based guideline is proposed

**SO_4^{2-} threshold is for taste, corrosion, and gastrointestinal effects. No health-based guideline is proposed for SO_4^{2-}

Table 2. Descriptive statistical data of the analyzed unconfined Quaternary groundwater samples

Parameters	Min.	Max.	Mean	S.D.	EPA, 2018	WHO, 2011	EHA, 2007
pH	7.89	8.23	8.13	0.14	6.5-8.5	6.5-8.5	6.5-8.5
EC	11.46	12.45	11.98	0.41	--	--	--
TDS	7678.00	8342.00	8023.60	276.77	500	1000	1000
Ca^{2+}	712.00	801.00	770.00	34.02	--	--	--
K^{+}	12.00	15.00	13.40	1.14	--	--	--
Mg^{2+}	37.50	47.00	41.96	3.64	--	--	--
Na^{+}	1875.00	2084.00	1989.20	74.66	200	200*	200
HCO_3^{-}	122.00	146.00	137.40	9.32	--	--	--
Cl^{-}	2622.67	3127.63	2959.25	196.37	250	250*	250
NO_3^{2-}	116.33	185.92	151.74	30.00	10	50	45
SO_4^{2-}	1684.42	1900.40	1803.93	79.91	250	500**	250
Al	0.00	0.21	0.05	0.09	0.05-0.2	0.1	--
Ba	0.02	0.03	0.03	0.01	2	0.7	0.7
Cr	0.02	0.03	0.02	0.00	0.1	0.05	0.05
PO_4	0.10	17.54	9.73	8.94	--	0.1	--
Cu	0.03	0.21	0.07	0.08	1.3	2	2
Fe	0.01	0.49	0.10	0.21	0.3	0.3	0.3
Pb	0	0.12	0.03	0.05	0.015	0.01	-
Mn	0.01	0.12	0.03	0.05	0.05	0.4	0.4
Zn	0.02	0.18	0.07	0.06	5	3	3

Concentrations and TDS are in ppm, temperature is in temperature is in °C, and EC is in mmhos/cm. Guidelines for water quality of drinking water (Egyptian Health Authority, 2007; Environmental Protection Agency of Water, 2018; WHO, 2011)

*Taste threshold only, no health-based guideline is proposed

** SO_4^{2-}threshold is for taste, corrosion, and gastrointestinal effects. No health-based guideline is proposed for SO_4^{2-}

Table 3. Descriptive statistical data of the analyzed Miocene groundwater samples.

Parameters	Min.	Max.	Mean	S.D.	EPA, 2018	WHO, 2011	EHA, 2007
pH	**7.38**	**8.23**	**7.81**	**0.25**	**6.5-8.5**	**6.5-8.5**	**6.5-8.5**
EC	**0.56**	**3.52**	**1.59**	**0.87**	**--**	**--**	**--**
TDS	**357.00**	**2250.00**	**1015.69**	**553.68**	**500**	**1000**	**1000**
Ca^{2+}	**46.51**	**281.02**	**102.76**	**80.97**	**--**	**--**	**--**
K^{+}	**4.00**	**11.00**	**8.08**	**1.71**	**--**	**--**	**--**
Mg^{2+}	**15.55**	**46.75**	**31.13**	**7.72**	**--**	**--**	**--**
Na^{+}	**39.00**	**357.00**	**171.92**	**93.55**	**200**	**200***	**200**
HCO_3^{-}	**160.00**	**273.00**	**214.38**	**33.30**	**--**	**--**	**--**
F^{-}	**0.07**	**0.29**	**0.17**	**0.07**	**2**	**1.5**	**2**
Cl^{-}	**59.10**	**598.89**	**275.01**	**144.26**	**250**	**250***	**250**
NO_3^{2-}	**0.10**	**3.56**	**1.14**	**1.09**	**10**	**50**	**45**
SO_4^{2-}	**28.00**	**565.00**	**162.23**	**189.63**	**250**	**500****	**250**
Al	**0.00**	**0.18**	**0.02**	**0.05**	**0.05-0.2**	**0.1**	**--**
Ba	**0.02**	**0.10**	**0.03**	**0.03**	**2**	**0.7**	**0.7**
Cr	**0.01**	**0.02**	**0.01**	**0.01**	**0.1**	**0.05**	**0.05**
Co	**0.00**	**0.01**	**0.01**	**0.01**	**--**	**--**	**--**
Cu	**0.00**	**0.03**	**0.01**	**0.01**	**1.3**	**2**	**2**
Fe	**0.02**	**0.27**	**0.06**	**0.07**	**0.3**	**0.3**	**0.3**
Mn	**0.01**	**0.14**	**0.04**	**0.04**	**0.05**	**0.4**	**0.4**
Zn	**0.01**	**0.04**	**0.02**	**0.01**	**5**	**3**	**3**

Concentrations and TDS are in ppm, temperature is in °C, and EC is in mmhos/cm. Guidelines for water quality of drinking water (Egyptian Health Authority, 2007; Environmental Protection Agency of Water, 2018; WHO, 2011)
*Taste threshold only, no health-based guideline is proposed
** SO_4^{2-} threshold is for taste, corrosion, and gastrointestinal effects, no health-based guideline is proposed for SO_4^{2}

Table 4. Classification of water according to salinity (Mayer et al., 2005).

Salinity (ppm)	Salinity status	Category
<500	Fresh	Drinking and irrigation
500-1,000	Marginal	Irrigation
1,000-2,000	Brackish	Irrigation with caution
2,000-5,000	Moderately saline	Primary drainage
5,000-10,000	Saline	Secondary drainage and saline groundwater
10,000-35,000	Highly saline	Very saline groundwater
>35,000	**Brine**	**Seawater**

a- Major ions

Regarding the concentrations of the major cations, the maximum Na^{+} concentrations in the semi-confined Quaternary aquifer exceed the EPA (2018), WHO (2011), and EHA (2007) guidelines for drinking water by about 1.5 times, while it is higher by about 1.8 times in the Moghra aquifer. On the other hand, the maximum Na^{+} concentrations in the unconfined Quaternary aquifer exceed the EPA (2018), WHO (2011), and EHA (2007) guidelines for drinking water by about 10.42 times (Tables 1, 2, and 3). Additionally, Cl^{-} and SO_4^{2-} maxima showed higher

values compared to the EPA (2018) standards by 2.3 and 1.5 folds; respectively (Table 1) for the semi-confined Quaternary aquifer and higher by 2.4 and 2.2 folds; respectively (Table 2) for the unconfined Quaternary aquifer, while they exceed the limits by 12.5 and 7.6 folds; respectively for the Miocene Quaternary (Table 3).On the other hand, the deep Nubian aquifer water sample analysis shows that the Na^+ concentration increases by 125 times the EPA (2018), WHO (2011), and EHA (2007) guidelines for the drinking water, while the Cl- concentration increases by 214 times the EPA (2018), WHO (2011), and EHA(2007) guidelines.

b- *Minor ions and trace elements*

The NO_3^{2-} maxima of the groundwater of the semi-confined Quaternary aquifer exceeds the EPA (2018) permissible limits by 1.3 folds while F^- showed a normal range from 0.07 to 0.73 ppm (Tables 1 and S1). The unconfined Quaternary aquifer NO_3^- maximum concentration exceeds the EPA (Environmental Protection Agency of Water, 2018) permissible limit by ~4 folds (Table 2). The Moghra aquifer NO_3^{2-} and F^- concentrations ranged from 0.1 to 3.56 ppm and from 0.07 to 0.29 ppm; respectively, that showed a normal range for the drinking water (Tables 3 and S1). Additionally, the semi-confined Quaternary aquifer chemical analysis showed that the maximum concentrations of Ba, Mn, Fe, Cr exceed the WHO (2011) permissible limits by about 0.3, 6.5, 1.5, and 1.4 folds; respectively (Table 1), while the concentrations of Cu (0-0.02 ppm) and Zn (0.01-0.14 ppm) conform to drinking water quality standards (Tables 1 and S1). Co and V concentrations (0-0.01 ppm) and (0-0.04 ppm); respectively, have no health-based standard limits (Tables 1 and S1). On the other hand, the Moghra aquifer chemical analysis showed that the concentrations of Al, Ba, Cr, Cu, Fe, Mn, and Zn conform to drinking water quality standards, which are (0-0.18 ppm), (0.02-0.1 ppm), (0.01-0.02 ppm), (0-0.03 ppm), (0.02-0.27 ppm), (0.01-0.14 ppm), and (0.01-0.04 ppm); respectively (Tables 3 and S1), showing that all of these elements are below the guidelines of the EHA (2007). The unconfined Quaternary aquifer chemical analysis showed that the maximum concentrations of Al, and Fe exceed the WHO (2011) permissible limits by about 2.1 and 1.6 folds; respectively (Table 2), while the concentrations of Ba (0.02-0.03 ppm), Cr (0.02-0.03 ppm), Cu (0.03-0.21 ppm), Mn (0.01-0.12 ppm), and Zn (0.02-0.18 ppm) conform to drinking water quality standards (Tables 2 and S1). PO_4 maximum concentration is excessively higher than the WHO (2011) standards by ~175 folds while Pb increases by about 12 folds (Table 2). Finally, the deep Nubian aquifer water analysis shows an increase in Fe concentration about 7.5 folds than the EPA (2018), WHO (2011), and EHA (2007) guidelines for the drinking water (Table S1), while the Nubian aquifer chemical analysis showed that the concentrations of Al, Ba, Cr, Cu, Mn, and Zn conform to drinking water quality (Table S1).

4.2. Bivariate statistical analysis

a- Pearson correlation

The Pearson Correlation Coefficient "r" was used to estimate the relations between ions in the semi-confined Quaternary and the Miocene aquifers, where the findings are shown in (Tables S2 and S3). The semi-confined Quaternary aquifer water samples showed a positive correlation of Na^+ (0.990), Ca^{2+} (0.986), Cl^- (0.977), Mg^{2+} (0.947), SO_4^{2-}(0.936), K^+ (0.910), and HCO_3^- (0.696) with TDS as these ions are accountable for the salinity. A positive correlation exists between potassium and the major ions Cl^- (0.931), Mg^{2+} (0.895), Na^+ (0.893), SO_4^{2-} (0.786), and HCO_3^- (0.685) and Mn (0.539). This could be due to the effect of chemical fertilizers as one of most common nutrients is potassium chloride (KCl) that is essential for plant development. It is a low-cost supply of K^+ for most crops, and it is used directly as a component of NPK fertilizers (Roy et al., 2006). The strong positive correlation of sodium with Cl^-

(0.97) may be due to the presence of fertilizers such as the chloride-containing fertilizers such as KCl (47 percent Cl), NP/NPK complexes of KCl composition, NaCl (60 percent Cl), and ammonium chloride (66 percent Cl) (Roy et al., 2006). The positive correlation of Cr with Co (0.548), and Ni (0.539) could be due to mixed sources (geogenic/anthropogenic) effects as Cr is found in nature at low concentrations, so it is produced from natural processes (e.g., from the ferromagnesium minerals within the Nile valley soil (El-Anwar et al., 2019) or human activities. Ca^{2+} and SO_4^{2-} (0.912) have a strong positive association, which could be linked to the use of agricultural gypsum ($CaSO_4.H_2O$). Agricultural gypsum is used as a natural fertilizer to enhance the physical and chemical properties of soils (Chen & Dick, 2011). Gypsum is applied as an amendment that works to remove excess exchangeable sodium from the root zone while also improving the soil's physical qualities (Roy et al., 2006). Bicarbonate shows a moderate positive correlation with Cl^- (0.651), Mg^{2+} (0.644), Ba (0.55), SO_4^{2-} (0.544), and Mn (0.519), which could be related to fertilizers, and the use of nutrient fertilizers like manganese carbonate, one of the Mn fertilizers used for soil amendments (Roy et al., 2006).

On the other hand, the Miocene aquifer water samples showed a positive correlation of TDS with the ions responsible for the salinity Cl^- (0.97), Na^+ (0.97), SO_4^{2-} (0.96), Ca^{2+} (0.95), Mg^{2+} (0.9), and HCO_3^- (0.61). As no rock in the nature can produce nitrate ion, the NO_3^- is mainly originated from an anthropogenic source (Bakari et al., 2012), so, the positive correlation of alkalinity with NO_3^- (0.6) and sodium (0.69) indicates the presence of nitrate fertilizers as KNO_3 (Hall, 2018). The positive correlation of chromium with Co (0.97), Cu (0.74), and Zn (0.67) and negative correlation of F^- (-0.79) indicate linking with other heavy metals that suggest the presence of anthropogenic sources, while the positive correlation with HCO_3^- (0.66), Na^+ (0.54), and Mg^{2+} (0.58) indicate the presence of fertilizers as the Egyptian organic fertilizers that have a wide range of total chromium content, ranging from 275 to 660 mg/kg (Sroor et al., 1999). The negative correlation with pH (0.56) indicates the acidic effect of Cr on the groundwater (McGrane, 2021).

Evaporation enriches fluorine in groundwater, which is derived from rock-water interactions. The principal process impacting the chemical composition of groundwater in a high fluoride area is the evaporative concentration (Sun et al., 2019). The negative correlation of F^- with Cl^- (-0.55), NO_3^- (-0.6), Cr (-0.79), Co (-0.76), Cu (-0.6), Zn (-0.54), Mg^{2+} (-0.51), and HCO_3^- (-0.59) indicates that these ions limit the increasing of F^-.

HCO_3^- provides a positive correlation with Cl^-, NO_3^-, SO_4^{2-}, Cr, Co, and Zn indicating anthropogenic effects as for soil or plant applications, mixed and compound fertilizers comprise N, P, K, Fe, Mn, Zn, and/or Cu in various forms (FAO, 2005). Iron displays a positive correlation with EC, TDS, Ca^{2+}, Mg^{2+}, Na^+, Cl^-, SO_4^{2-}, and Al indicating the presence of a source of Fe (Abdelhameed et al., 2019). The positive correlation of Zn with other heavy elements (Cr, Cu, Co) indicates that these elements could be originated from anthropogenic sources.

4.3. Multivariate statistical analysis

a- Factor analysis (FA)

Statistical factor analysis is a familiar method to reduce large variables into significant factors using a satisfactory rotation of loadings (Abu Salem et al., 2017; 2022; Kaiser, 1958). Factor analysis was applied to the semi-confined Quaternary and the Miocene aquifers' water analyses where the Kaiser-Meyer-Olkin (KMO) and Bartlett's sphericity tests were first applied to check the reliability of applying the factor analysis. After that, a varimax rotation with Principal Component Analysis (PCA) extraction method was made (Tables 5 and 6).

Table 5. The Kaiser-Meyer-Olkin (KMO), Bartlett's sphericity tests and the factor analysis for the examined semi-confined Quaternary aquifer groundwater samples.

KMO and Bartlett's Test			
Kaiser-Meyer-Olkin Measure of Sampling Adequacy.			0.645
Bartlett's Test of Sphericity	Approx. Chi-Square		339.238
	Df		66
	Sig.		0
Rotation sums of squared loadings	Total	8.280	1.916
	% of Variance	68.998	15.964
	Cumulative %	68.998	84.963
		1	2
	EC	0.991	-0.112
	TDS	0.991	-0.113
	Ca^{2+}	0.983	-0.074
	Na^{+}	0.978	-0.115
	Cl^{-}	0.978	-0.005
	Mg^{2+}	0.947	-0.105
	K^{+}	0.937	0.162
	SO_4^{2-}	0.898	-0.336
	HCO_3^{-}	0.760	0.309
	F^{-}	-0.106	-0.782
	Ni	-0.513	0.595
	Fe	-0.027	0.813

Extraction Method: Principal Component Analysis.
Rotation Method: Varimax with Kaiser Normalization.

Table 6. The Kaiser-Meyer-Olkin (KMO), Bartlett's sphericity tests and the factor analysis for the examined Miocene aquifer groundwater samples.

KMO and Bartlett's Test				
Kaiser-Meyer-Olkin Measure of Sampling Adequacy.				0.536
Bartlett's Test of Sphericity	Approx. Chi-Square			216.023
	Df			55
	Sig.			0.000
Rotation sums of squared loadings	Total	5.365	2.499	1.481
	% of Variance	48.770	22.716	13.467
	Cumulative %	48.770	71.486	84.953
		1	2	3
	TDS	0.940	0.298	0.141
	Na^{+}	0.839	0.475	0.226
	Cl^{-}	0.912	0.303	0.183
	Mg^{2+}	0.871	0.324	0.077
	SO_4^{2-}	0.928	0.197	0.085
	Ca^{2+}	0.965	0.087	0.047
	HCO_3^{-}	0.416	0.747	0.024
	F^{-}	-0.294	-0.825	0.033
	K^{+}	0.356	0.153	0.689
	Ba	-0.022	0.045	0.847
	NO_3^{-}	0.096	0.822	0.409

Extraction Method: Principal Component Analysis.
Rotation Method: Varimax with Kaiser Normalization.

The KMO of the semi-confined aquifer water samples is 0.645 indicating that the examined variables contribute to a common variance. Two factors were extracted based on eigenvalues more than one describing most of the variability in the studied samples, with a total cumulative variance of ~84.96 percent (Table 5 and Fig. 4a), while the KMO of the Miocene aquifer water samples is 0.536 where three factors were extracted to describe most of the variability, with a total cumulative variance of ~ 84.95 percent (Table 6 and Fig. 4b). Furthermore, the findings of Bartlett's sphericity test applied on the semi-confined Quaternary aquifer water samples were Chi-Square = 339.238; degree of freedom = 66; and p 0.001 "=zero", while it gave the results of Chi-Square = 216.023; degree of freedom = 55; and p 0.001 "=zero" for the Miocene aquifer water samples indicating that the examined variables contribute to a common variance.

For the semi-confined Quaternary aquifer water samples; the first factor represents ~ 69% of the total variance. It shows strong positive loadings on TDS (0.991), EC (0.991), Ca^{+2} (0.983), Na^{+} (0.978), Cl^{-} (0.978), Mg^{2+}, K^{+} (0.947), SO_4^{2-} (0.898), and HCO_3^{-} (0.760) which could be termed the salinity factor. The second factor provides positive loading on Fe (0.813), and Ni (0.595), and strong negative loading on F^{-} (-0.782) and could be termed the iron factor confirmed by the presence of hematite mineral as a source of iron in the clay lenses within the Quaternary aquifer (Abdelhameed et al., 2019).

On the other side, the FA analysis applied to the Miocene aquifer water samples provided three factors. The first factor showed strong positive loadings on Ca^{2+} (0.965), TDS (0.940), SO_4^{-2} (0.928), Cl^{-} (0.912), Mg^{2+} (0.871), and Na^{+} (0.839)]. It could be termed the salinity factor. The second factor is characterized by a strong positive loading on HCO_3^{-} (0.747) and NO_3^{-} (0.822) and a strong negative loading on F^{-} (-0.825). It could be termed the recharge factor. Additionally, the third factor showed strong and moderate loadings on Ba (0.847) and K^{+} (0.689); respectively. It could be termed the geogenic factor.

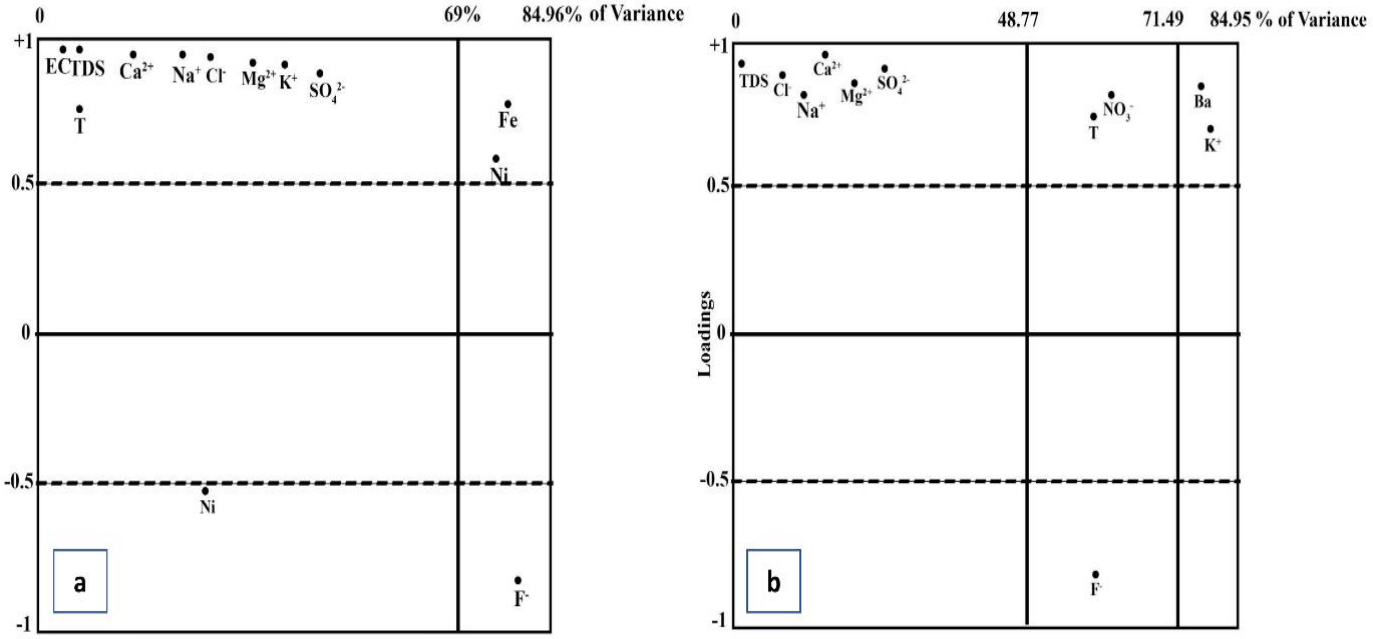

Fig. 4. Extracted factors using varimax rotation, a) for the semi-confined Quaternary aquifer water samples and b) for the Miocene aquifer water samples.

a- Hierarchical cluster analysis

According to Davis and Sampson, (1986), one of the well-known methods for identifying various classes and groupings within the data under investigation is the Hierarchical Cluster Analysis (HCA) which can display the findings with a dendrogram representation. To eliminate mistakes caused by the orders of magnitude and the variance of the variables, the dataset was normalized before performing HCA to the Z scores for the semi-confined Quaternary aquifer data and standardized by the range from 1 to -1 for the Miocene aquifer data. To determine clusters in the dataset of the semi-confined Quaternary and Miocene aquifers' water samples, a phenon line at distance 10 was drawn (Figs. 5 and 6). Accordingly, two main clusters were defined for both aquifers each of them splits into two sub-groups (Figs. 5,6, and 7).

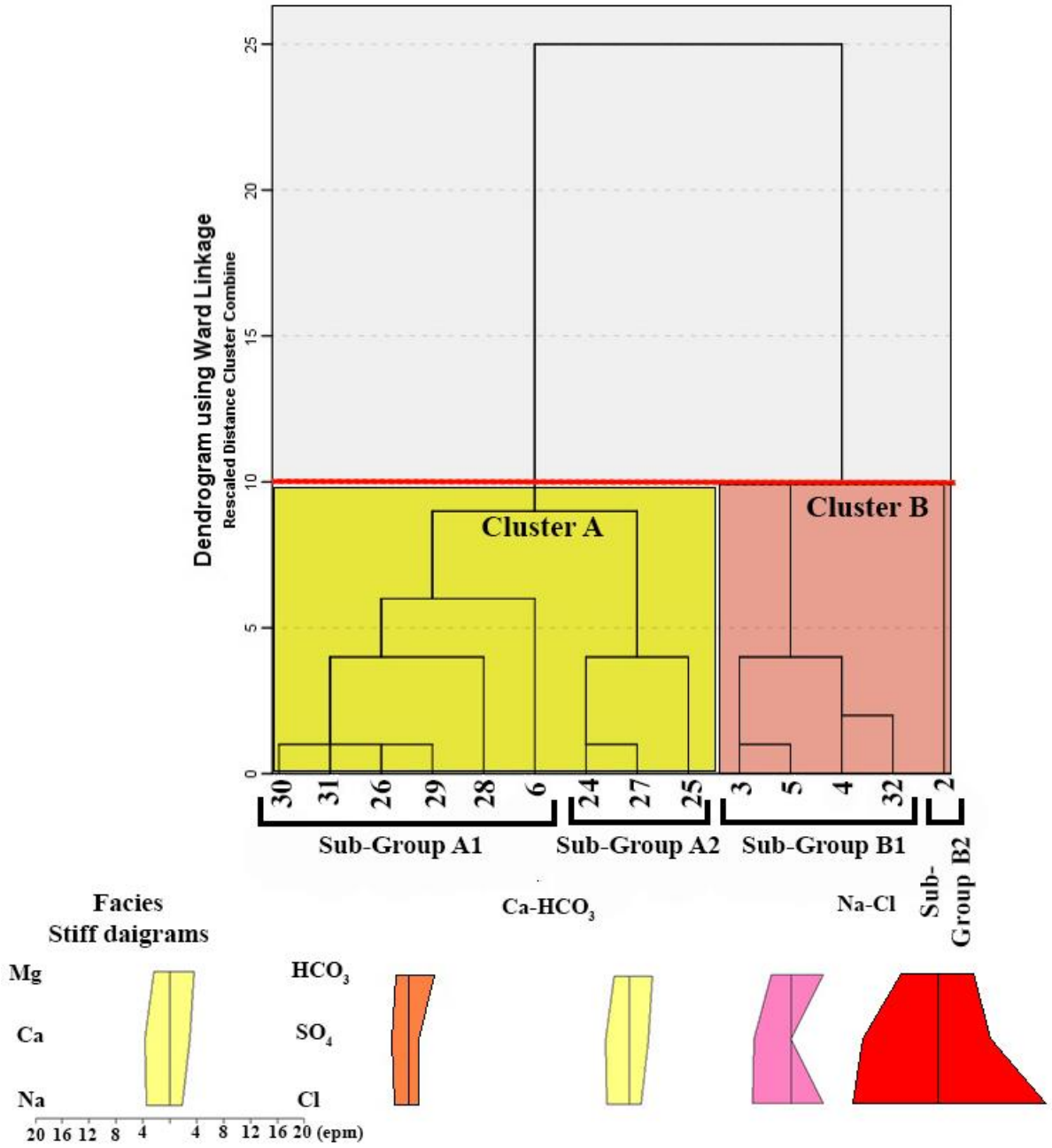

Fig. 5. Dendrogram of the semi-confined Quaternary aquifer groundwater samples based on Hierarchical Cluster Analysis (HCA). The phenon line is represented by the dashed red line.

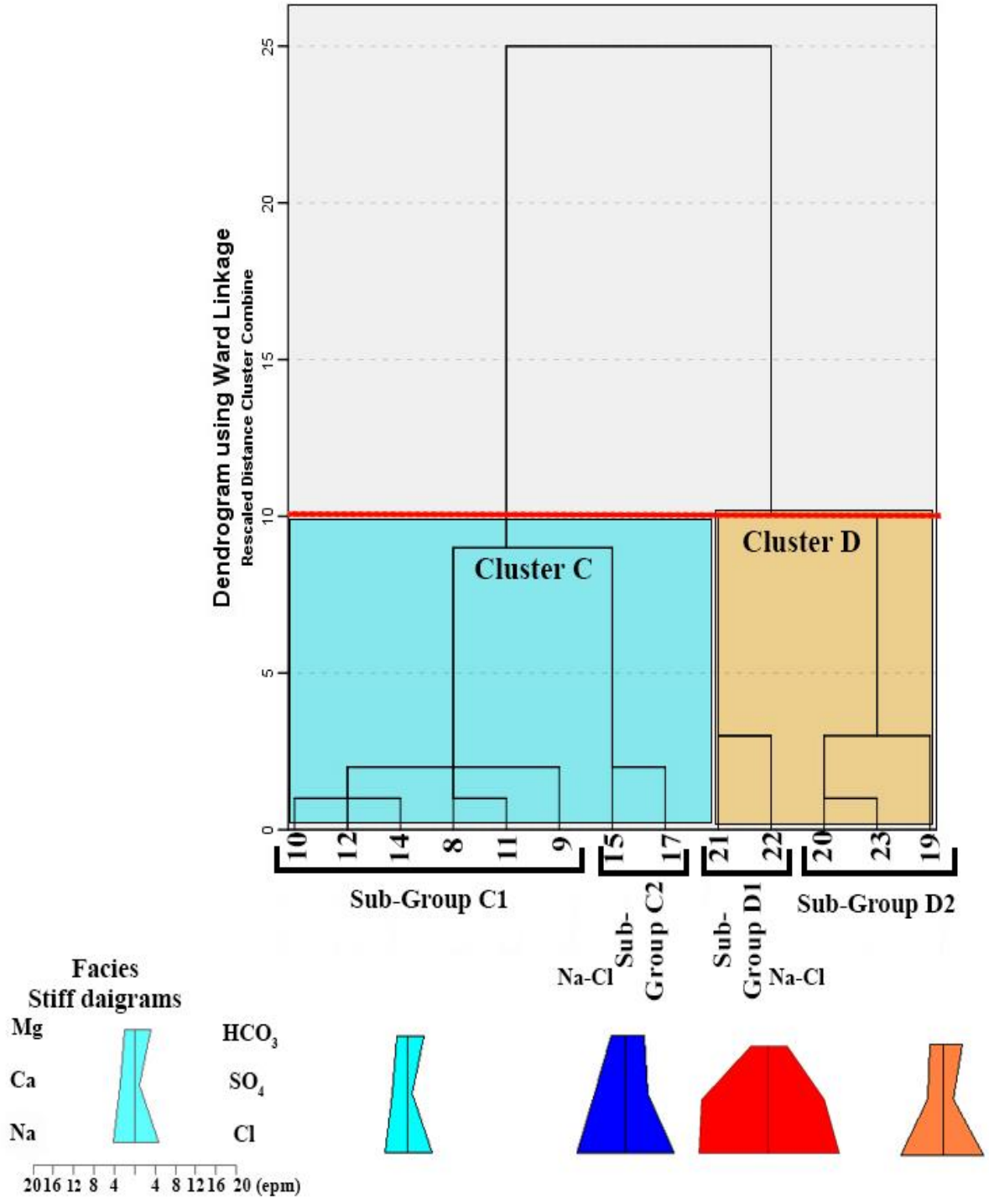

Fig. 6. Dendrogram of the Miocene aquifer groundwater samples based on Hierarchical Cluster Analysis (HCA). The phenon line is represented by the dashed red line.

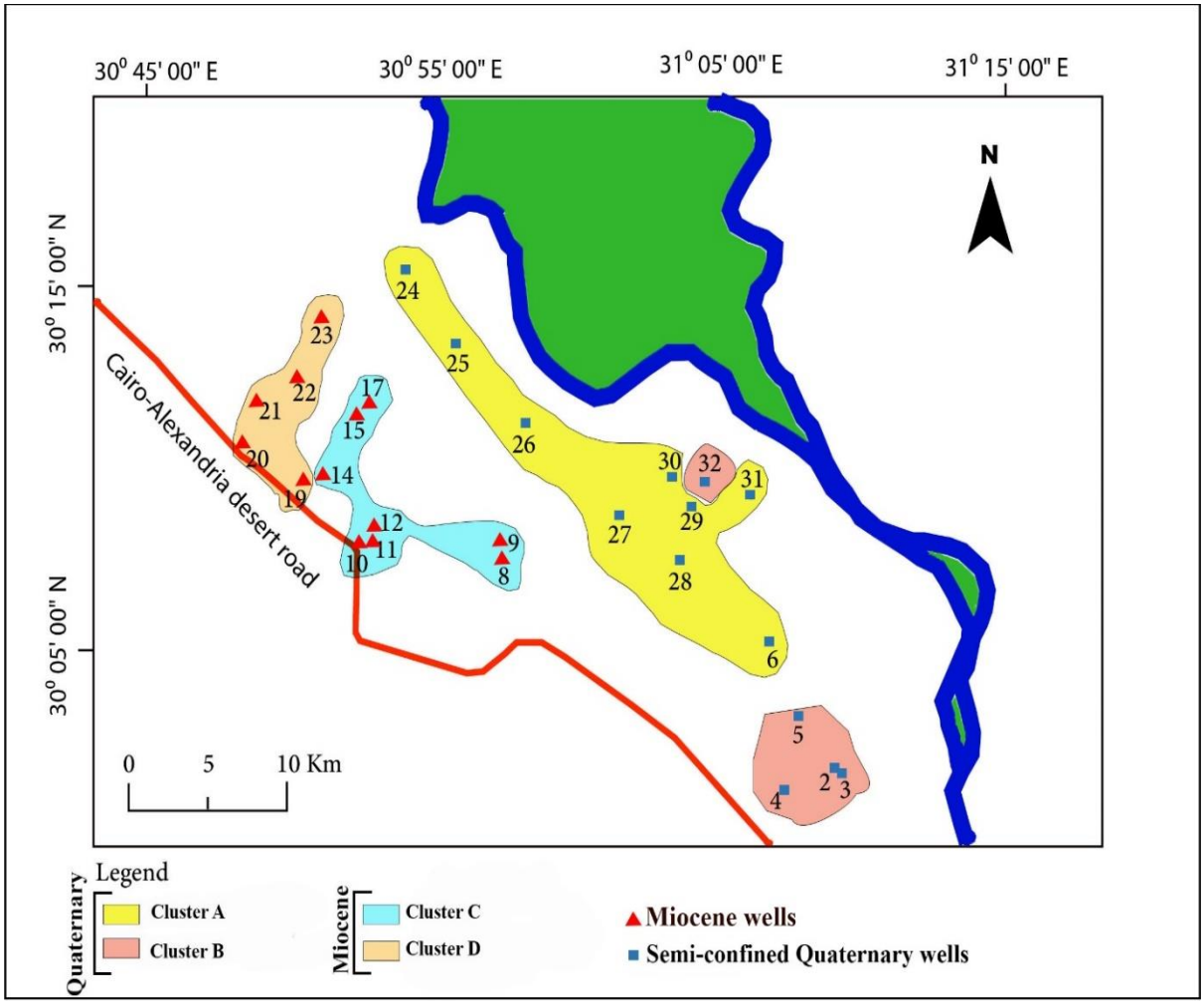

Fig. 7. Clusters distribution for the semi-confined Quaternary and the Miocene aquifers' water samples.

The main clusters representing the semi-confined Quaternary aquifer (Groups A and B) were divided into A1, A2, B1, and an independent case (B2), while those of the Miocene aquifer (Group C and D) were subdivided into C1, C2, D1, and D2. Stiff diagrams (Figs. 5 and 6) were used to illustrate the ionic predominance between subgroups by displaying the mean concentrations of each sub-group. The minima, maxima, and averages of the studied variables for each sub-group analyzed by HCA were shown in Tables 7 and 8.

Both sub-groups of the first cluster (A) are dominated by Ca-HCO_3 facies while the rest of clusters (B), (C), and (D) are characterized by Na-Cl facies. The spatial distribution of each cluster distinguished for the semi-confined Quaternary and the Miocene aquifers is given in Figure (7).

Table 7. Descriptive statistics of the main distinguished sub-groups for the analyzed semi-confined Quaternary aquifer water samples (Concentrations and TDS are in ppm, EC is in mmhos/cm).

	A1			A2			B1			B2
	Min.	**Max.**	**Mean**	**Min.**	**Max.**	**Mean**	**Min.**	**Max.**	**Mean**	**Independent case**
pH	7.71	8.18	7.903	7.66	7.76	7.713	7.92	7.99	7.945	7.890
EC	0.5	1.06	0.725	0.89	1.17	0.993	1.47	2.12	1.540	3.090
TDS	321	678	463.167	568	749	635.667	685	1357	986.000	1975.000
HCO_3^-	175	274	226.667	175	244	221.000	268	340	300	326.000
Ca^{2+}	41	76.43	54.572	68.25	78	73.823	85	135	114.673	230.000
K^+	5	8	6.833	6	7	6.333	8	10	8.750	16.000
Mg^{2+}	17	33	24.868	24	33	29.00	26.5	51.51	37.485	69.980
Na^+	30	94	50.667	64	100	79.667	70	220	136.750	300.000
F^-	0.12	0.19	0.167	0.07	0.73	0.333	0.14	0.3	0.185	0.150
Cl^-	25.86	88	52.255	58	73.49	66.830	81	308.9	176.725	575.000
NO_3^-	0.1	3.69	0.730	28.9	57.29	39.477	0.1	0.22	0.130	3.000
SO_4^{2-}	23.73	147	68.438	88.44	242.25	141.563	147.22	285	209.455	375.000
Ba	0.1	0.15	0.117	0.07	0.21	0.150	0.2	0.24	0.218	0.120
Cr	0.006	0.071	0.024	0.16	0.17	0.017	0.007	0.018	0.010	0.006
Co	0.002	0.014	0.011	0.007	0.009	0.013	0.002	0.012	0.005	0.002
Cu	0.003	0.01	0.007	0.007	0.009	0.008	0.003	0.021	0.012	0.003
Fe	0.11	0.46	0.297	0.01	0.02	0.013	0.21	0.38	0.273	0.230
Mn	0.44	1.59	1.010	0.06	0.24	0.153	0.87	1.89	1.653	1.740
Ni	0.002	0.013	0.011	0.002	0.009	0.004	0.002	0.007	0.003	0.002
V	0.001	0.012	0.009	0.017	0.036	0.024	0.001	0.011	0.004	0.001
Zn	0.019	0.14	0.039	0.02	0.036	0.024	0.009	0.022	0.014	0.012

Table 8. Descriptive statistics of the main distinguished sub-groups for the analyzed Miocene aquifer water samples (Concentrations and TDS are in ppm, EC is in mmhos/cm).

	C1			C2			D1			D2		
	Min.	**Max.**	**Mean**	**Min.**	**Max.**	**Mean**	**Min.**	**Max.**	**Mean**	**Min.**	**Max.**	**Mean**
pH	7.62	8.23	7.913	7.74	8.1	7.92	7.57	7.64	7.61	7.38	7.85	7.67
EC	0.558	1.2	0.969	1.4	2.29	1.845	3.06	3.52	3.29	1.49	1.56	1.513
TDS	357	770	621.5	898	1466	1182	1957	2250	2103.5	953	998	968
HCO_3^-	160	209	187.333	214	235	224.5	219	273	246	219	263	240.667
Ca^{2+}	46.51	81.8	59.342	89.82	145.96	117.89	269.9	281.02	275.46	49.88	80.2	64.36
K^+	4	9	7.5	8	11	9.5	2	9	8.5	7	10	8
Mg^{2+}	15.55	30.13	25.342	32.07	32.07	32.07	41.31	46.75	44.03	30.9	37	33.3
Na^+	39	138	95.333	147	275	211	300	357	328.5	180	210	194.667
F^-	0.19	0.29	0.237	0.1	0.22	0.16	0.12	0.14	0.13	0.07	0.12	0.09
Cl^-	59.1	241.8	169.867	245.8	399	322.4	455	598.89	526.945	225.71	337	285.737
NO_3^-	0.1	0.58	0.358	1	2.85	1.925	0.86	1.74	1.3	0.59	3.56	2.083
SO_4^{2-}	28	59	48.733	125	288	206.5	557	565	561	50.36	140	93.843
Al	0.007	0.015	0.0107	0.008	0.012	0.01	0.002	0.181	0.092	0.002	0.002	0.004
Ba	0.016	0.032	0.024	0.091	0.1	0.096	0.026	0.026	0.026	0.018	0.027	0.021
Cr	0.007	0.008	0.007	0.007	0.007	0.007	0.015	0.016	0.016	0.018	0.02	0.019
Co	0.002	0.002	0.002	0.002	0.002	0.002	0.011	0.014	0.013	0.013	0.014	0.013
Cu	0.003	0.003	0.003	0.003	0.003	0.003	0.007	0.009	0.008	0.006	0.027	0.014
Fe	0.015	0.094	0.042	0.023	0.065	0.044	0.095	0.267	0.181	0.017	0.083	0.04
Mn	0.01	0.069	0.032	0.12	0.135	0.128	0.027	0.032	0.03	0.016	0.02	0.018
Zn	0.008	0.019	0.015	0.017	0.027	0.022	0.023	0.023	0.023	0.021	0.041	0.029

The comparison between the different subgroups of each cluster indicates that the average concentrations of the variables of subgroup A2 showed increased TDS, Na^+, Cl^-, NO_3^-, SO_4^{2-}, and Ba than subgroup A1, while subgroup A1 showed increased Fe and Mn than subgroup A2. Additionally, subgroup B2 showed increased TDS, Ca^{2+}, K^+, Mg^{2+}, Na^+, Cl^-, NO_3^-, SO_4^{2-} than subgroup B1 (Table 7). It is noted that although sample 32 is closer to cluster A, it is assigned to

cluster B as it is of shallower depth than those in cluster A (Fig. 7).

Moreover, subgroup C2 showed higher TDS, HCO_3^-, Ca^{2+}, Na^+, Cl^-, SO_4^{2-}, and slightly higher Mn and NO_3^- than subgroup C1 (Table 8). Subgroup D1 showed higher TDS, Ca^{2+}, Na^+, Cl^-, SO_4^{2-}, and Fe than subgroup D2, while subgroup D2 showed increased NO_3^- than subgroup D1 (Table 8).

4.4. Hydrogeochemical processes controlling groundwater chemistry

4.4.1. Hydrochemical facies

To investigate the hydrochemical facies of the studied groundwater samples, we used Piper diagram (Piper, 1944).

Most of the semi-confined Quaternary aquifer water samples (71.5%) and the Miocene aquifer water samples (69.2%) plot on the mixed zone (Fig. 8) and are characterized by mixed Ca-Mg-Cl water type, while about (21.4%) of the semi-confined Quaternary aquifer water sample plot on the secondary alkalinity (A2) field showing a Ca-Mg-HCO_3 water type that could represents surface water recharge, and only about 7.1% of the semi-confined Quaternary aquifer water samples belong to Ca-Mg-Cl-SO_4 water type of secondar salinity property (S2) (Fig. 8). The rest of the Miocene aquifer water samples split to about 15.4% belonging to Na-Cl type of primary salinity property (S1) and 15.4% belonging to Ca-Mg-Cl-SO_4 type (S2) (Fig. 8). Both the deep Nubian aquifer water sample and the unconfined Quaternary aquifer samples belong to the Na-Cl type (S_1). The variability of the samples from the semi-confined Quaternary aquifer from Ca-Mg-Cl-SO_4 type (S2) to mixed Ca-Mg-Cl type then Ca-Mg-HCO_3 type (A2) point to a hydrochemical changes along the flow direction (from southeast to northwest) (Fig. 3a and Fig. 8, samples along the blue arrow). In contrast, the Miocene aquifer water chemistry changes from Ca-Mg-Cl-SO_4 type (S2) to mixed Ca-Mg-Cl type and finally to Na-Cl type (S1) along the flow direction (from northeast to southwest) (Fig. 3b and Fig. 8, samples along the red arrow).

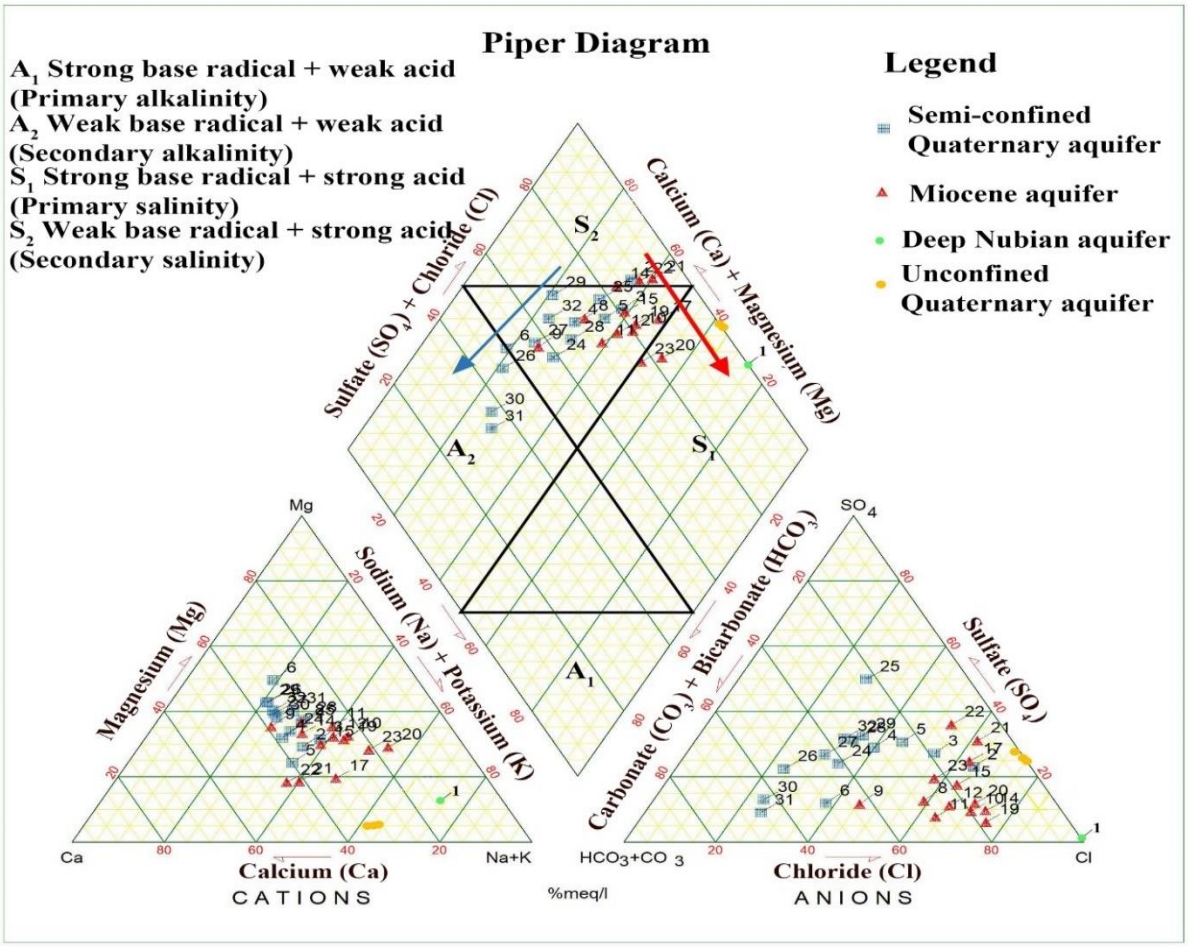

Fig. 8. Piper diagram (Piper, 1944), displaying the different hydrogeochemical classes of the Quaternary aquifer, the Miocene, and the deep Nubian aquifers water samples. The blue and red arrows indicate the chemical changes along the flow direction in the semi-confined Quaternary and the Miocene aquifers; respectively.

4.4.2. Hydrochemical processes controlling groundwater chemistry

a- Gibbs diagram

Gibb's diagram is used to distinguish the different hydrogeochemical processes such as evaporation, rock-water interaction, and precipitation by plotting a ratio of (Na+K)/(Na+K+Ca) or Cl/(Cl+HCO_3) in epm versus the TDS (ppm) (Gibbs, 1970; Nosair et al., 2022). The diagram is divided into three areas according to the hydrogeochemical process affecting the groundwater composition (Fig. 9 a and b). Accordingly, the water samples collected from the semi-confined Quaternary aquifer plot in the rock weathering section representing the chemical interaction between the groundwater and the host rock, while the unconfined Quaternary aquifer plot in the evaporation section. On the other hand, the majority of the groundwater samples from the Miocene aquifer plot at the rock weathering section, and the rest of the samples plot in the evaporation zone, while the Nubian aquifer water sample plot out of Gibb's diagram nutshell (Fig. 9 a and b).

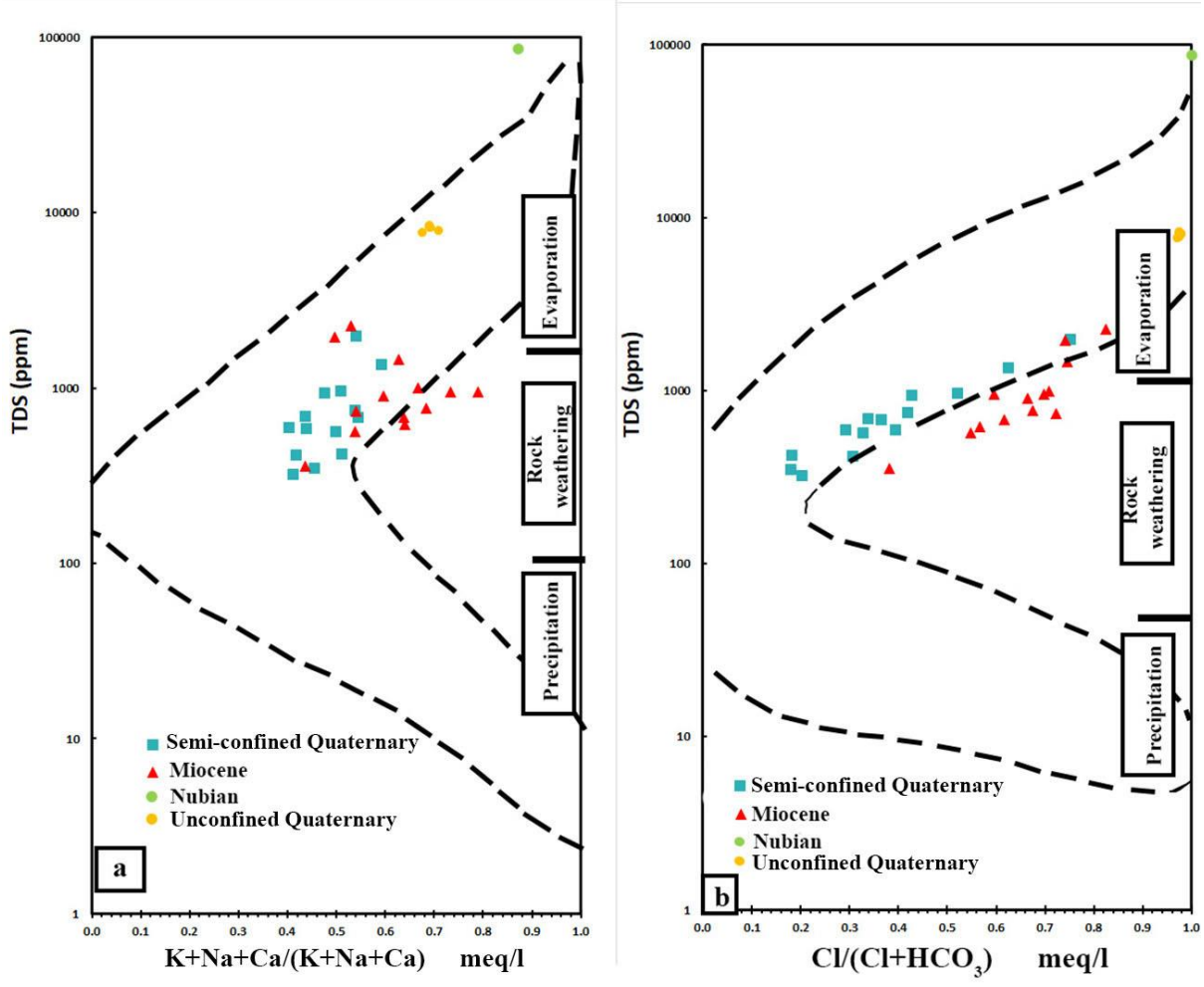

Fig. 9. Gibb's diagram showing the hydrogeochemical processes affecting the different groundwater chemistry.

b- Evaporation

The bivariate relation between the ratio of Na^+/Cl^- versus the electrical conductivity EC (Fig. 10a) gives an indication whether the samples are controlled by evaporation when the EC increases without change in Na^+/Cl^- ratio (Jankowski & Acworth, 1997) or due to silicate weathering and/or ion exchange when Na^+/Cl^- ratio increases at nearly lower EC (Nkotagu, 1996).

The Na^+/Cl^- ratio of the studied samples ranges from 0.67 to 2.25. The semi-confined Quaternary aquifer water samples showed increasing Na^+/Cl^- ratio at lower EC signifying the silicate weathering/ ion exchange processes, while the Miocene aquifer water samples display low Na^+/Cl^- ratio with low salinity ranges (357- 2250 ppm) (Fig. 10a). The unconfined Quaternary aquifer water samples have low Na^+/Cl^- ratio at very high salinity ranges (7678-8342 ppm) while the sample from the Nubian aquifer shows very high salinity at Na^+/Cl^- ratio at less than one (Fig. 10a) indicating that evaporation could be a possible process affecting the water chemistry in these aquifers as discussed in Gibbs diagram.

c- Silicate weathering

The plotting of $HCO_3^-+SO_4^{-2}$ against $Ca^{2+}+Mg^{2+}$ (Fig. 10b) indicates whether the groundwater is controlled by carbonate and evaporite weathering (e.g., calcite, dolomite, and gypsum) when the ratio $Ca^{2+}+Mg^{2+}/SO_4^{2-}+HCO_3^-$ equals to one, by ion exchange or silicate weathering when the ratio is less than one, and by reverse ion exchange when the ratio is more than one (Cerling et al., 1989; Fisher & Mullican, 1997; Kumar et al., 2009). The majority of the semi-confined Quaternary aquifer water samples plots below the 1:1 line indicating that silicate weathering and/ or ion exchange play a role in the water chemistry of this water (Fig. 10b). Conversely, the majority of the Miocene aquifer and all the samples from the unconfined Quaternary aquifer and the sample from Nubian aquifer plot over a 1:1 line which indicates an excess of $Ca^{2+}+Mg^{2+}$ over $SO_4^{2-}+HCO_3^-$ that could be due to reverse ion exchange (Fig. 10b).

Additionally, a relation between Cl^- versus Na^+ can signify if the chemistry of the water samples is controlled by halite dissolution (on the equiline), reverse ion exchange (below the equiline), or silicate weathering (above the equiline) (Jacks et al., 1999; Loni et al., 2015; Srinivasamoorthy et al., 2008) (Fig. 10c). Most of the semi-confined and the unconfined Quaternary aquifer water samples lie above the 1:1 line indicating silicate weathering, while the majority of the Miocene aquifer water samples plotted below the 1:1 line indicating reverse ion exchange and reused irrigation water (Fig. 10c). The sample from the Nubian aquifer lie below the equiline indicating reverse ion exchange reactions controlling the chemistry of this water (Fig. 10c). According to Garrels (1976), clay minerals weathering is responsible for the elevated sodium, calcium, and magnesium concentrations in groundwater in addition to the dissolving of limestone, dolomite, gypsum, and anhydrite. Few samples from the Miocene aquifer show the effect of silicate weathering.

d- Ion exchange reactions

One of the methods that give an indication for ion/ reverse ion exchange processes is the chloro-alkaline indices (CAI). Schoeller (1977) proposed it where it has been utilized by various researchers to find the ion exchange processes that influence groundwater chemistry (Aghazadeh & Mogaddam, 2011; Toumi et al., 2015; Zhu et al., 2007). The following equation is used to get the chloro-alkaline index (1) (CAI 1):

$$CAI\ 1 = (Cl^- - (Na^+ + K^+))/Cl^-$$

When Na^+ and K^+ in water exchange with Ca^{2+} and Mg^{2+} in the rocks (reverse ion exchange process), the CAI 1 diagram displays a positive index value, whereas when Ca^{2+} and Mg^{2+} in water exchange with Na^+ and K^+ in the rocks, the CAI 1 diagram shows a negative index value (ion exchange process). Nearly all the semi-confined and the unconfined Quaternary aquifer water samples lie in the negative region of the CAI 1 diagram indicating the samples affected by ion exchange processes, while about 50% of the Miocene aquifer water samples and the Nubian water sample lie in the positive region of the diagram that represents reverse ion exchange processes and the rest

of the samples plotted in the positive field of the diagram (Fig. 10d). These results were also previously confirmed by the relations in figures (10 b and c).

e- Evaporite / carbonate dissolution reactions

By plotting a scatter diagram between Ca^{2+} versus SO_4^{2-}, the plot of samples along the 1:1 line indicates the effect of gypsum dissolution (Essamin & Kamel, 2018). Nearly all the collected water samples from the semi-confined, the Miocene, and the Nubian aquifers plot above the 1:1 line indicating a Ca source possibly from reverse ion-exchange reaction resulting from desorption of Ca^{2+} into the water or from gypsum amendments for cultivation (Ettazarini, 2005) (Fig. 10e). The samples from the unconfined Quaternary aquifer plot nearly at the equiline suggesting gypsum dissolution.

Even more, establishing a relationship between Cl^- and SO_4^{2-} may deduce an anthropogenic effect on the groundwater, in which the elevation of Cl^- concentration over SO_4^{2-} might be assigned to irrigation water reuse and/or sewage contamination, where the increase of SO_4^{2-} over Cl^- is mostly due to the use of gypsum as an agricultural amendment (Subramani et al., 2010). All of the Miocene, the Nubian, and the unconfined Quaternary aquifer and about 50% of the semi-confined Quaternary aquifer water samples showed an increase of Cl^- over SO_4^{2-} (over 1:1 line), and the remainder of the semi-confined Quaternary aquifer water samples showed an increase of SO_4^{2-} over Cl^- (Fig. 10f). This indicate that the Cl chemistry of most groundwater samples could be controlled by irrigation water reuse and/ or sewage contamination while the chemistry of the rest of the groundwater samples from the semi-confined aquifer are affected by gypsum applications in cultivation.

In a bivariate relationship between HCO_3^- and Ca^{2+} in meq/l, calcite and dolomite dissolution control samples if they lie between the 1:2 and 1:4 lines, while if they plot above the 1:4 line, they could be associated with anthropogenic activities, gypsum dissolution, and/or reverse ion exchange reaction. The plot of samples below the 1:2 line could be related to biological processes and/or CO_2 dissolution in water (Sonkamble et al., 2012) (Fig. 10 g) and equation (1):

$$CO_2 + H_2O = H_2CO_3 = H^+ + HCO_3^- \quad (1)$$

Most of the groundwater samples of the semi-confined Quaternary aquifer and the Miocene aquifer plot below the 1:2 line, indicating that calcite and/ or dolomite dissolution does not control the calcium and bicarbonate concentrations in the samples and favoring the possibility of biological activities or CO_2 dissolution water in addition to the possibility of a meteoric recharge to both aquifers, while the unconfined Quaternary and the Nubian aquifer water samples lie above 1:4 line indicating the possibility of gypsum dissolution and /or reverse ion exchange (Fig. 10g).

According to the preceding discussion, the chemistry of the semi-confined Quaternary aquifer water is affected by silicate weathering and/ or ion exchange reactions, gypsum applications in cultivation and the return flow from irrigation water in addition to meteoric recharge. The chemistry of the unconfined Quaternary aquifer water samples is affected by evaporation, silicate weathering and/ or ion exchange reactions, gypsum applications in cultivation and the return flow from irrigation water. Additionally, the groundwater from the Miocene aquifer is affected by reverse ion exchange reactions, reuse of irrigation water and gypsum applications in addition to meteoric recharge. The Nubian groundwater is affected by evaporation and reveres ion exchange.

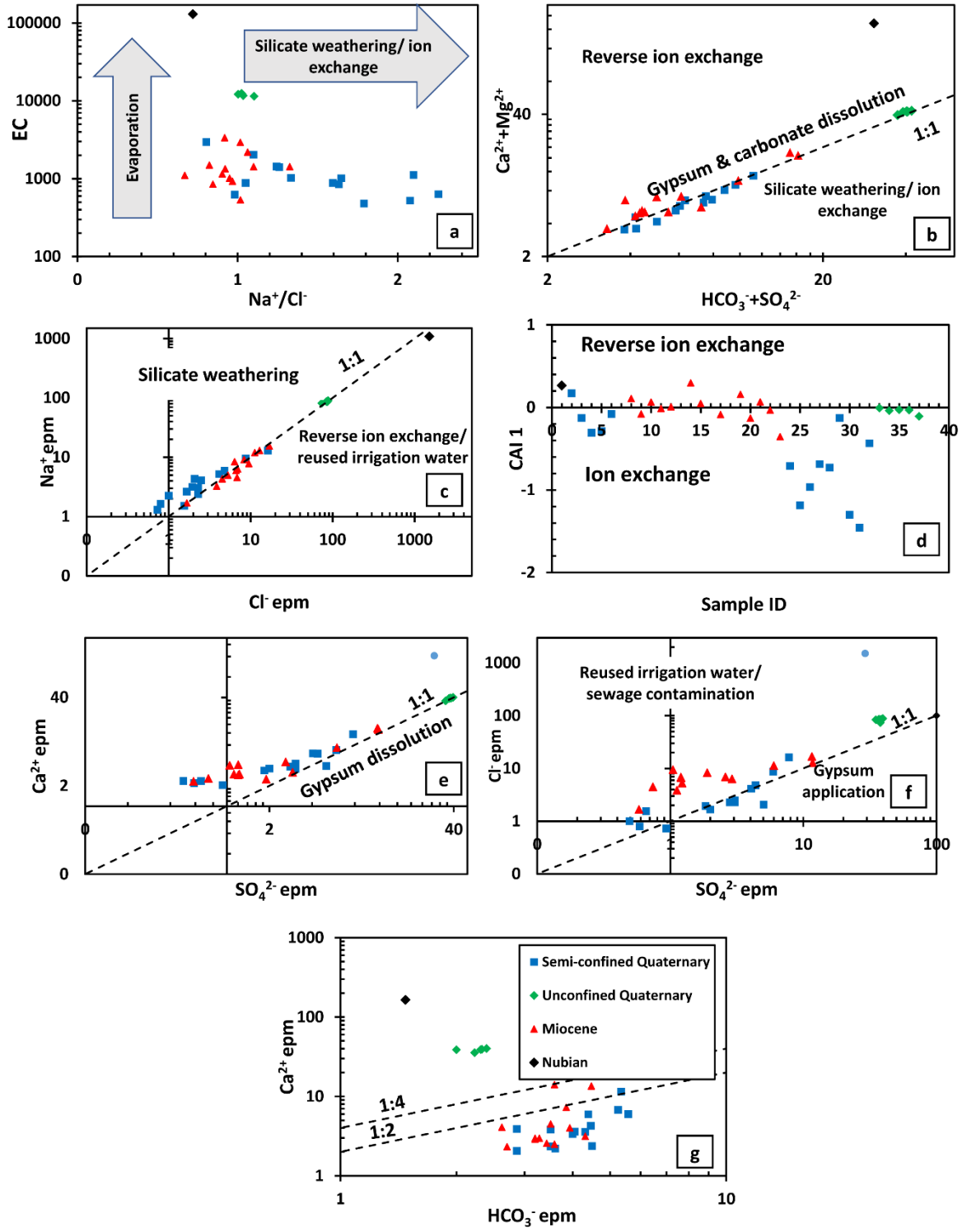

Fig. 10. Bivariate relations between the different ions in groundwater samples.

e- Saturation indices

The groundwater can dissolve or precipitate minerals according to their saturation indices as they regulate the equilibrium between the aqueous solution and the host rock (Mohamed et al., 2015; Nosair et al., 2022; Redwan et al., 2016). The SI is a relation between the ions' activity product and the thermodynamics reaction constants (Clark & Fritz, 1997; Domenico, 1972; Domenico & Schwartz, 1997; Drever, 1997). The saturation index (SI) was calculated using the PHREEQC interactive code by applying the following equation (Parkhurst & Appelo, 2013):

$$SI = \log [\text{ion activity product}]/K_T$$

Where: K_T is the equilibrium constant at temperature T. Both the semi-confined and the unconfined Quaternary, the Miocene, and the Nubian aquifer water samples show oversaturation with calcite and dolomite (Fig. 11 a and b), while they express an undersaturation with respect to gypsum and halite (Fig. 11 c and d).

The semi-confined Quaternary aquifer water samples are slightly oversaturated with respect to barite at low salinities (indicating the enrichment of barium in this water), while that of the unconfined Quaternary aquifer approaches saturation (Fig 11e). The groundwater of the Miocene aquifer is undersaturated with respect to barite up to 1000 ppm then it becomes near saturation at high salinity, while the Nubian is undersaturated with barite (Fig. 11e).

Finally, the majority of the semi-confined Quaternary aquifer samples show an oversaturation with respect to siderite and rhodochrosite (Fig. 11 f and g) indicating the enrichment of iron and manganese in this water, while the unconfined Quaternary, Miocene, and the Nubian aquifer groundwaters are undersaturated with respect to rhodochrosite and siderite (Fig. 11 f and g).

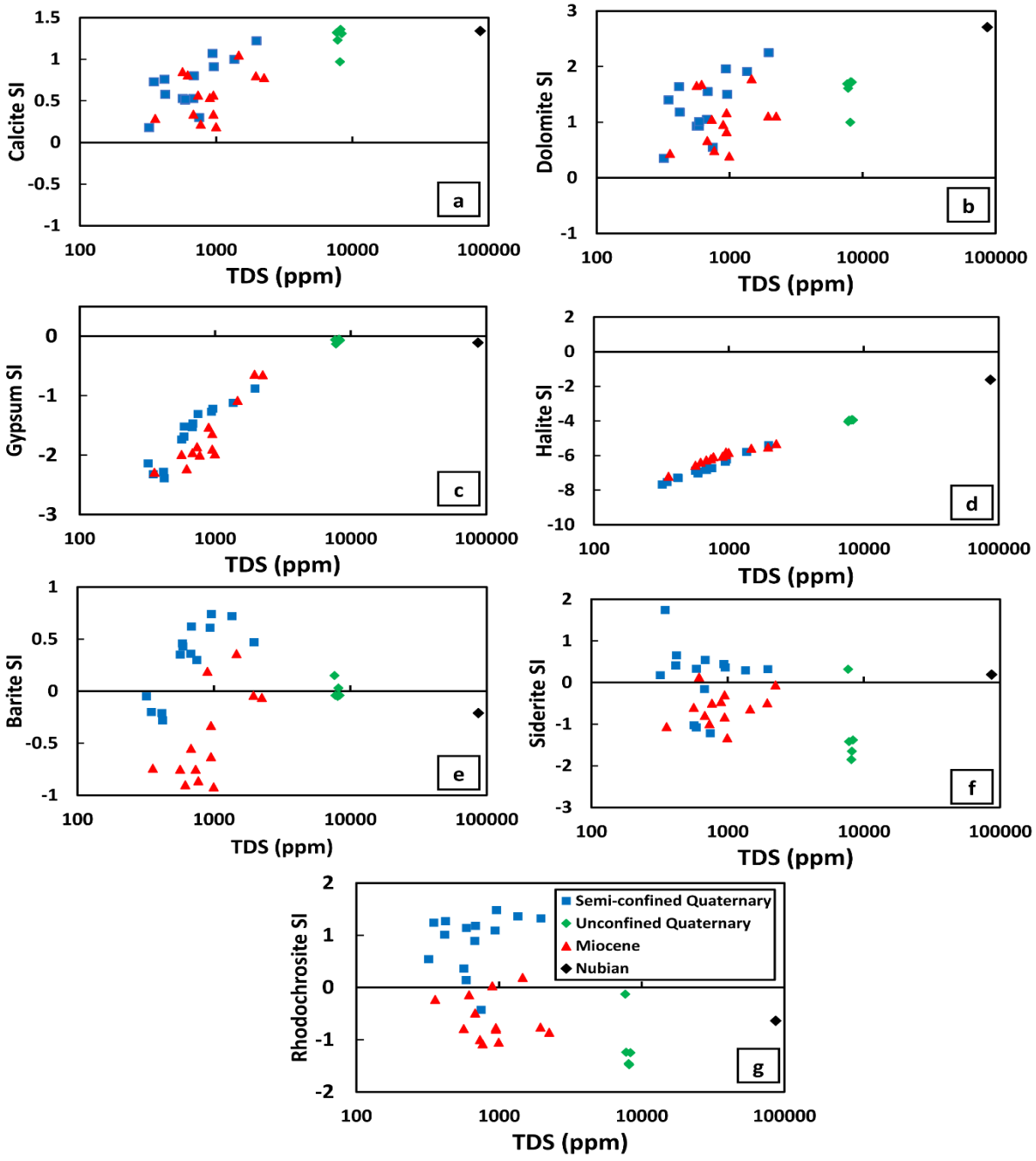

Fig. 11. Saturation indices of the semi-confined and the unconfined Quaternary, and the Miocene aquifers a) barite, b) calcite, c) dolomite, d) gypsum, e) halite, f) rhodochrosite, and g) siderite.

4.4.3 Water quality changes through time

Both the semi-confined Quaternary and the Miocene aquifers groundwater samples were analyzed through two periods; 2021 (Table S1) and 2018 (Table S4) (Mohallel, 2020), where changes in water quality are represented by box–whisker plots (Figs. 12 and 13). Boxplot is a visual representation of numerical data expressing different statistical parameters such as; minimum, first quartile, median, third quartile, and mean (Larsen, 1985). The salinity and the average concentrations of major ions in the groundwater from the semi-confined Quaternary aquifer decrease from 2018 to 2021, while the nitrate average concentration increases through time (Fig. 12). The increase of the nitrate average concentration may be due to the usage of fertilizers containing nitrate compounds such as; KNO_3 (Hall, 2018) while the decrease in the TDS and the major ions could be due to the continuous recharge from the River Nile. On the other hand, in the Miocene aquifer chemical analysis, the salinity and the major ions average concentrations increase from 2018 to 2021 except SO_4^{2-} and NO_3^- (Fig. 13). The salinity increase of the groundwater could be due to over-pumping.

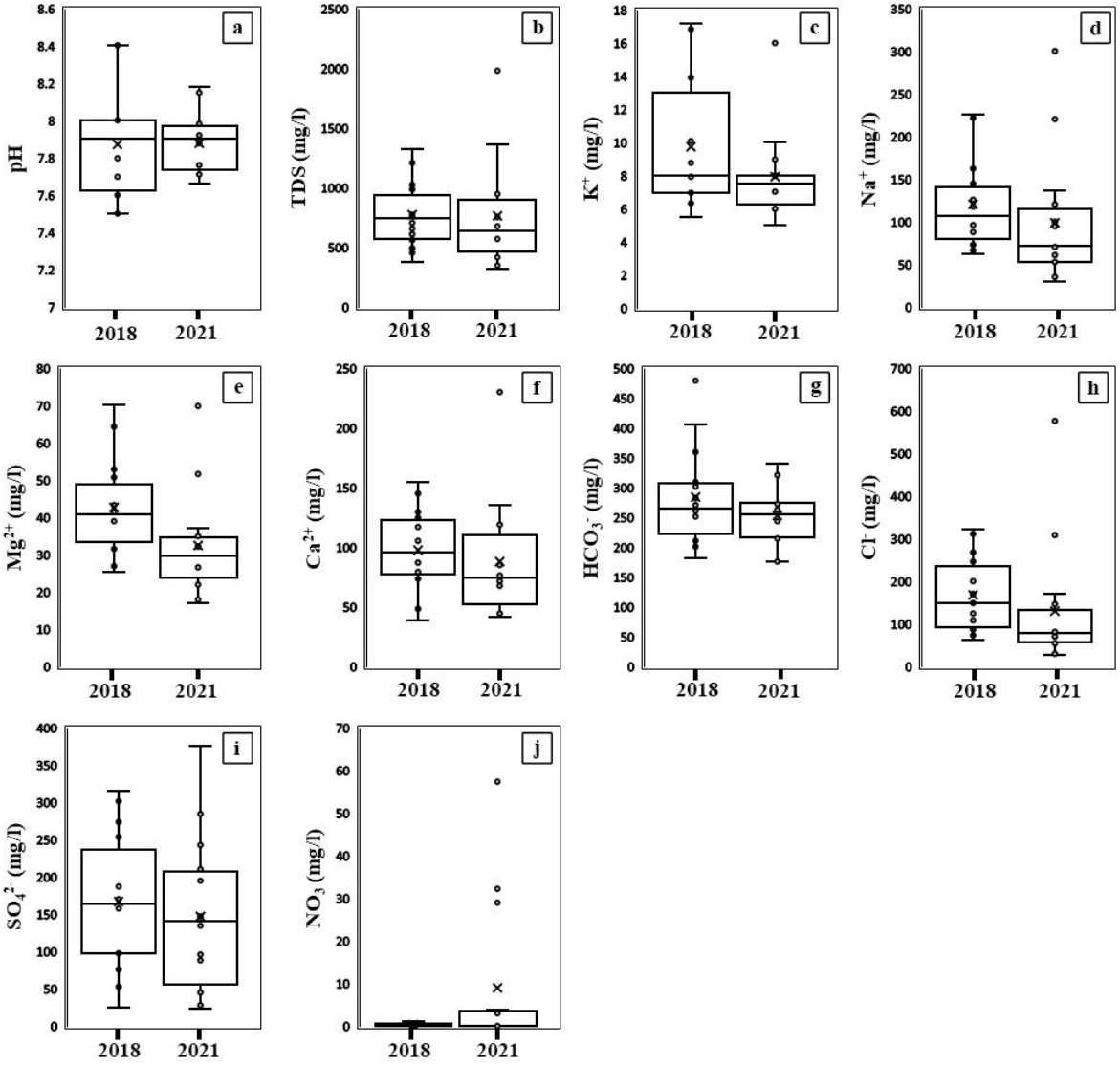

Fig. 12 Box-Whisker plot representation for the chemical analysis during the two periods; 2021 and 2018 (Mohallel, 2020) through different variables in the semi-confined Quaternary aquifer water samples a) pH, b) TDS, c) K^+, d) Na^+, e) Mg^{2+}, f) Ca^{2+}, g) HCO_3^-, h) Cl^-, i) SO_4^{2-}, and j) NO_3^-.

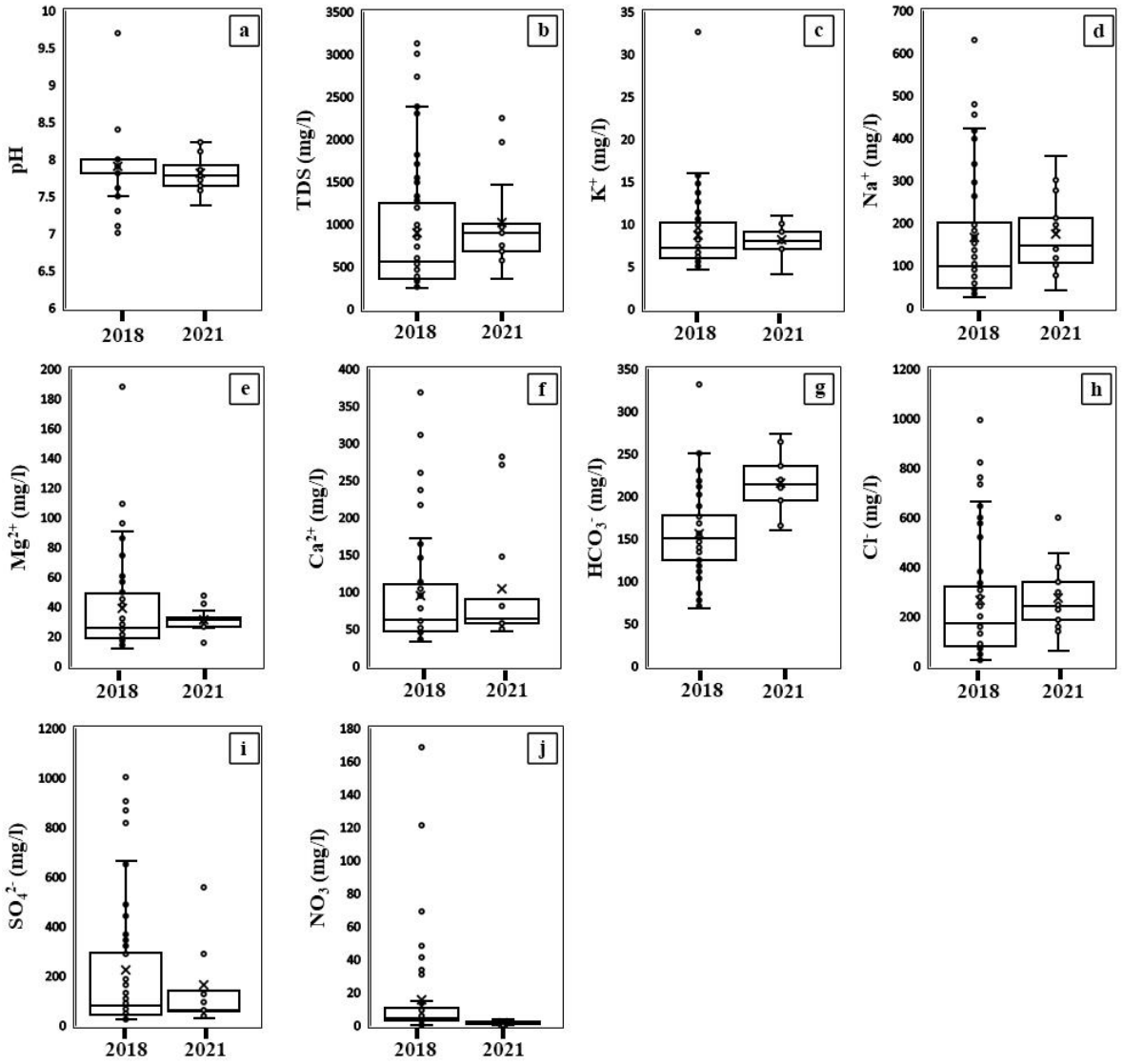

Fig. 13. Box-Whisker plot representation for the chemical analysis during the two periods; 2021 and 2018 (Mohallel, 2020) through different variables in the Miocene aquifer water samples a) pH, b) TDS, c) K^+, d) Na^+, e) Mg^{2+}, f) Ca^{2+}, g) HCO_3^-, h) Cl^-, i) SO_4^{2-}, and j) NO_3^-.

5. Conclusions

The Hydrogeochemistry study of the four aquifers in the Abu Roash area and its environs in this study is based mainly on statistical analysis, bivariate plots, Piper and Gibb's diagrams. First, the statistical analysis of the semi-confined Quaternary aquifer showed that the groundwater is affected by different types of fertilizers such as chemical chloride-containing fertilizers and the use of nutrient fertilizers like manganese carbonate, in addition to the anthropogenic effects. Additionally, factor analysis provided iron factor due to the presence of iron in the clay lenses within the Quaternary aquifer. The Miocene aquifer statistical analysis indicated the influence of an anthropogenic effect that led to an increase in NO_3^- content in the groundwater as well as the influence of fertilizers such as the Egyptian organic fertilizers that have a wide range of total chromium content and chloride-containing fertilizers. Furthermore, factor analysis showed a recharge factor and a geogenic factor.

Second, bivariate plots demonstrated the different ions' relations for the unconfined Quaternary, the semi-confined Quaternary, and the Miocene aquifers. The semi-confined Quaternary aquifer water samples are affected by ion exchange and silicate weathering while calcite and /or dolomite dissolution do not control the calcium and bicarbonate concentrations in the samples. In the Miocene aquifer, bivariate plots show that the groundwater is subjected to a reverse ion-exchange reaction while higher bicarbonate concentrations may be due to biological processes or carbon dioxide dissolution. Additionally, the unconfined Quaternary aquifer bivariate plots show that the groundwater is subjected to reverse ion-exchange and evaporation as well as anthropogenic impacts.

Then, the classification of the groundwater for the four different aquifers obtained from Piper and Gibb's diagrams indicates that groundwater types of the semi-confined aquifer change with the direction of groundwater flow (from southeast to northwest) from Ca-Mg-Cl-SO_4 type to mixed Ca-Mg-Cl type then Ca-Mg-HCO_3 type, and represent a chemical interaction between the groundwater and the host rock, while the Miocene aquifer water types change with groundwater flow (from northeast to southwest) from Ca-Mg-Cl-SO_4 type to mixed Ca-Mg-Cl type and finally to Na-Cl type. The majority of the groundwater samples from the Miocene aquifer plot at the rock weathering section, while the rest of the samples plot in the evaporation zone. Contrariwise, the unconfined Quaternary and the deep Nubian aquifers groundwater belong to Na-Cl water type (S_1), and the unconfined Quaternary aquifer plot in the evaporation section, while the Nubian aquifer water sample lies out of Gibb's diagram zonation.

The hydrogeochemistry of the different aquifers indicates that the semi–confined Quaternary and the Moghra aquifers are best used for irrigation, while the unconfined Quaternary aquifer belongs to the Na-Cl water type and the deep Nubian aquifer water is brine. Finally, the comparison between the two periods for the semi-confined Quaternary and the Miocene aquifers using box-plots shows that the average salinity decreases from 2018 to 2021, while the nitrate average concentration increases through the time in the semi-confined Quaternary aquifer due to the usage of fertilizers containing nitrates. On the other hand, the Miocene aquifer chemical analysis shows increase in the salinity and the major ions average concentrations from 2018 to 2021 except SO_4^{2-} in addition to NO_3^- average concentrations decrease from 2018 to 2021. The increase of groundwater salinity of the Miocene aquifer could be due to excessive pumping and should be considered in future development plans in the west Delta area.

Ethics approval and consent to participate: This article does not contain any studies with human participants or animals performed by any of the authors.

Consent for publication: All authors declare their consent for publication.

Conflicts of Interest: The author declares no conflict of interest.

Contribution of Authors: All authors shared in writing, editing and revising the MS and agree to its publication.

Acknowledgement: The authors would like to thank the National Water Research Centre (NWRC) for facilitating the water analysis operations.

6. References

Abdel-Gawad, G. I., Saber, S. G., El Shazly, S. H., & Salama, Y. F. (2011) Turonian Rudist Facies from Abu Roash area, North Western Desert, Egypt. Journal of African Earth Sciences, 59(4–5), 359–372.

Abdelhafez, A. A., Metwalley, S. M., & Abbas, H. H. (2020) Water resources, types and common problems in Egypt. Technological and Modern Irrigation Environment in Egypt: Best Management Practices & Evaluation. Springer Nature, Switzerland AG, pp. 15–34.

Abdelhameed, A. T., Salem, Z. E., & Osman, O. M. (2019) Sedimentological characteristics of the quaternary

groundwater aquifer, northwestern Nile Delta, Egypt. Groundwater in the Nile Delta, 73, 161–186.

Abdin, A. E., & Gaafar, I. (2009) Rational water use in Egypt. Technological Perspectives for Rational Use of Water Resources in the Mediterranean Region.

Abu Salem, H. S., Abu Khatita, A., Abdeen, M. M., Mohamed, E. A., & El Kammar, A. M. (2017) Geo-environmental evaluation of Wadi El Raiyan Lakes, Egypt, using remote sensing and trace element techniques. Arabian Journal of Geosciences, 10, 1–24.

Abu Salem, H. S., Gemail, K. S., Junakova, N., Ibrahim, A., & Nosair, A. M. (2022) An Integrated Approach for Deciphering Hydrogeochemical Processes during Seawater Intrusion in Coastal Aquifers. Water, 14(7), 1165.

Aghazadeh, N., & Mogaddam, A. A. (2011) Investigation of hydrochemical characteristics of groundwater in the Harzandat aquifer, Northwest of Iran. Environmental Monitoring and Assessment, 176(1–4), 183–195. https://doi.org/10.1007/s10661-010-1575-4

Bakari, S. S., Aagaard, P., Vogt, R. D., Ruden, F., Johansen, I., & Vuai, S. A. (2012) Delineation of groundwater provenance in a coastal aquifer using statistical and isotopic methods, Southeast Tanzania. Environmental Earth Sciences, 66(3), 889–902. https://doi.org/10.1007/s12665-011-1299-y

Cerling, T. E., Pederson, B. L., & Von Damm, K. L. (1989) Sodium-calcium ion exchange in the weathering of shales: Implications for global weathering budgets. Geology, 17(6), 552–554.

Chen, L., & Dick, W. A. (2011) Gypsum as an agricultural amendment: General use guidelines. Ohio State University Extension.

Clark, I. D., & Fritz, P. (1997) Environmental isotopes in hydrogeology. CRC press.

Davis, J. C., & Sampson, R. J. (1986) Statistics and data analysis in geology (Vol. 646). Wiley New York.

Dawoud, M. A., Darwish, M. M., & El-Kady, M. M. (2005) GIS-based groundwater management model for Western Nile Delta. Water Resources Management, 19, 585–604.

Domenico, P. A. (1972) Concepts and models in groundwater hydrology. McGraw Hill, New York.

Domenico, P. A., & Schwartz, F. W. (1997) Physical and chemical hydrogeology. John wiley & sons.

Drever, J. I. (1997) The geochemistry of natural waters Prentice Hall. Inc, New York.

Egyptian Health Authority. (2007) Guideline for drinking water and household. http://extwprlegs1.fao.org/docs/pdf/egy83626.pdf 458.

El Alfy, M., Lashin, A., Abdalla, F., & Al-Bassam, A. (2017) Assessing the hydrogeochemical processes affecting groundwater pollution in arid areas using an integration of geochemical equilibrium and multivariate statistical techniques. Environmental Pollution, 229, 760–770.

El-Anwar, A., Mekky, H. S., Abdel Wahab, W., Asmoay, A. S., Elnazer, A. A., & Salman, S. A. (2019) Geochemical characteristics of agricultural soils, Assiut governorate, Egypt. Bulletin of the National Research Centre, 43(1), 1-9.

El Tahlawi, M. R., Farrag, A. A., & Ahmed, S. S. (2008) Groundwater of Egyptian environmental overview." Environmental Geology, 55, 639–652.

El-Etr, H., & El-Baz, F. (1979) Utilization of ASTP Photographs in the study of small structures in Abu Rawash and Wadi El-Natrun, Egypt. Apollo-Soyuz Test Project Summary Science Report. Volume II: Earth Observations and Photography, NASA SP-412.

El-Fakharany, Z. (2013) Environmental Impact Assessment of Artificial Recharge of Treated Wastewater on Groundwater Aquifer System Case study Abu-Rawash, Egypt. The Journal of American Science, 9(2), 309–315.

El-Rawy, M., Abdalla, F., & El Alfy, M. (2020) Water resources in Egypt. In the Geology of Egypt. Springer: Berlin, Germany.

Eltarabily, M. G., & Moghazy, H. E. M. (2021) GIS-based evaluation and statistical determination of groundwater geochemistry for potential irrigation use in El Moghra, Egypt. Environmental Monitoring and Assessment, 193(5), 306.

Emara, M. M., El Sabagh, I., Kotb, A., Turkey, A. S., & Husseen, D. (2007) Evaluation of drinking groundwater for the rural areas adjacent to the nearby desert of Giza governorate of Greater Cairo, Egypt. Environmental Security in Harbors and Coastal Areas: Management Using Comparative Risk Assessment and Multi-Criteria Decision Analysis, 379–394.

Environmental Protection Agency of Water, O. (2018) 2018 Edition of the Drinking Water Standards and Health Advisories Tables (EPA 822-F-18-001).

Essamin, R., & Kamel, S. (2018) Incrustation ability of geothermal waters of the Continental Intercalaire aquifer in the Grand Erg Oriental basin (Algeria and South Tunisia). Environmental Earth Sciences, 77(6). https://doi.org/10.1007/s12665-018-7398-2.

Ettazarini, S. (2005) Processes of water–rock interaction in the Turonian aquifer of Oum Er-Rabia Basin, Morocco. Environmental Geology, 49(2), 293–299.

FAO, F. (2005) Agriculture Organization of the United Nations, land and plant nutrition management service. Land and Water Development Division, Fertilizer Sector, in Fertilizer Use by Crop in Egypt, FAO, Rome TC/D/Y5863E/1/01.05/300

Fisher, R. S., & Mullican William F, I. I. I. (1997) Hydrochemical evolution of sodium-sulfate and sodium-chloride groundwater beneath the northern Chihuahuan Desert, Trans-Pecos, Texas, USA. Hydrogeology Journal, 5, 4–16.

Garizi, A. Z., Sheikh, V., & Sadoddin, A. (2011) Assessment of seasonal variations of chemical characteristics in surface water using multivariate statistical methods. International Journal of Environmental Science & Technology, 8, 581–592.

Garrels, R. M. (1976) A survey of low temperature water-mineral relations. In Interpretation of environmental isotope and hydrochemical data in groundwater hydrology.

Gibbs, R. J. (1970) Mechanisms controlling world water chemistry. Science, 170(3962), 1088–1090.

Hall, J. O. (2018) Nitrate-and nitrite-accumulating plants. In Veterinary Toxicology, Elsevier, pp. (941–946).

Ibrahem, S. M. M. (2020) Groundwater hydrology and characteristics of the tertiary aquifers, Northwest Cairo, Egypt. NRIAG Journal of Astronomy and Geophysics, 9(1), 420–432.

Jacks, G., Sefe, F., Carling, M., Hammar, M., & Letsamao, P. (1999) Tentative nitrogen budget for pit latrines–eastern Botswana. Environmental Geology, 38, 199–203.

Kaiser, H. F. (1958) The varimax criterion for analytic rotation in factor analysis. Psychometrika, 23(3), 187–200.

Khalek, M. L. A., El Sharkawi, M. A., Darwish, M., Hagras, M., & Sehim, A. (1989) Structural history of Abu Roash district, Western Desert, Egypt. Journal of African Earth Sciences (and the Middle East), 9(3–4), 435–443.

Kumar, M., Kumari, K., Singh, U. K., & Ramanathan, A. L. (2009) Hydrogeochemical processes in the groundwater environment of Muktsar, Punjab: conventional graphical and multivariate statistical approach. Environmental Geology, 57, 873–884.

Kumar, S. K., Chandrasekar, N., Seralathan, P., Godson, P. S., & Magesh, N. S. (2012) Hydrogeochemical study of shallow carbonate aquifers, Rameswaram Island, India. Environmental Monitoring and Assessment, 184, 4127–4138.

Larsen, R. D. (1985) Box-and-whisker plots. Journal of Chemical Education, 62(4), 302.

Li, P., Tian, R., Xue, C., & Wu, J. (2017) Progress, opportunities, and key fields for groundwater quality research under the impacts of human activities in China with a special focus on western China. Environmental Science and Pollution Research, 24, 13224–13234.

Loni, O. A., Zaidi, F. K., Alhumimidi, M. S., Alharbi, O. A., Hussein, M. T., Dafalla, M., AlYousef, K. A., & Kassem, O. M. K. (2015) Evaluation of groundwater quality in an evaporation dominant arid environment; a case study from Al Asyah area in Saudi Arabia. Arabian Journal of Geosciences, 8, 6237–6247.

Masoud, A. A. (2014) Groundwater quality assessment of the shallow aquifers west of the Nile Delta (Egypt) using multivariate statistical and geostatistical techniques. Journal of African Earth Sciences, 95, 123–137.

Mayer, X. M., Ruprecht, J. K., & Bari, M. A. (2005) Stream Salinity Status and Trends in South West Western Australia in Salinity and Land Use Impacts Series, vol. 38. Department of Environment, Perth, Australia.

McGrane, K. (2021) Acidic water: risks, benefits, and more. https://www.healthline.com/nutrition/acidic-water

Mfonka, Z., Kpoumié, A., Ngouh, A. N., Mouncherou, O. F., Nsangou, D., Rakotondrabe, F., Takounjou, A. F., Zammouri, M., Ngoupayou, J. R. N., & Ndjigui, P.-D. (2021) Water Quality Assessment in the Bamoun Plateau, Western-Cameroon: Hydrogeochemical Modelling and Multivariate Statistical Analysis Approach. Journal of Water Resource and Protection, 13(2), 112–138.

Mohallel, S. A. (2020) Hydrogeochemical approach to evaluate groundwater quality in the area between Abu Rawash and El Khatatba, Northwest Cairo, Egypt. Current Science International, 09, (109-139).

Mohamed, E. A., El-Kammar, A. M., Yehia, M. M., & Salem, H. S. A. (2015) Hydrogeochemical evolution of inland lakes' water: A study of major element geochemistry in the Wadi El Raiyan depression, Egypt. Journal of Advanced Research, 6(6), 1031–1044.

Mohammed, A. M., Krishnamurthy, R. V, Kehew, A. E., Crossey, L. J., & Karlstrom, K. K. (2016) Factors affecting the stable isotopes ratios in groundwater impacted by intense agricultural practices: A case study from the Nile Valley of Egypt. Science of the Total Environment, 573, 707–715.

Mohammed, M. S., Elbeih, S. F., Mohamed, E. A., Abu Salem, H., Ibrahim, M., & ElSayed, E. E. (2022) Spectral Indices Based Study to Evaluate and Model Surface Water Quality of Beni Suef Governorate, Egypt. Egyptian Journal of Chemistry, 65(10), 631–645.

Nkotagu, H. (1996) The groundwater geochemistry in a semi-arid, fractured crystalline basement area of Dodoma, Tanzania. Journal of African Earth Sciences, 23(4), 593–605.

Nosair, A. M., Shams, M. Y., AbouElmagd, L. M., Hassanein, A. E., Fryar, A. E., & Abu Salem, H. S. (2022) Predictive model for progressive salinization in a coastal aquifer using artificial intelligence and hydrogeochemical techniques: A case study of the Nile Delta aquifer, Egypt. Environmental Science and Pollution Research, 29(6), 9318–9340.

Omar, M. M. M. (2021) Groundwater flow model of the quaternary aquifer in El Khatatba area for water resources management. Egyptian Journal of Pure and Applied Science, 58(1):51-61.

Parkhurst, D. L., & Appelo, C. A. J. (2013) Description of input and examples for PHREEQC version 3—a computer program for speciation, batch-reaction, one-dimensional transport, and inverse geochemical calculations. US Geological Survey Techniques and Methods, 6(A43), 497.

Piper, A. M. (1944) A graphic procedure in the geochemical interpretation of water-analyses. Eos, Transactions American Geophysical Union, 25(6), 914–928.

Redwan, M., Abdel Moneim, A. A., & Amra, M. A. (2016) Effect of water–rock interaction processes on the hydrogeochemistry of groundwater west of Sohag area, Egypt. Arabian Journal of Geosciences, 9, 1–14.

Roy, R. N., Finck, A., Blair, G. J., & Tandon, H. L. S. (2006) Plant nutrition for food security. A Guide for Integrated Nutrient Management. FAO Fertilizer and Plant Nutrition Bulletin, 16(368).

Jankowski, J., & Acworth, R. I. (1997) Impact of debris-flow deposits on hydrogeochemical processes and the developement of dryland salinity in the Yass River

Catchment, New South Wales, Australia. Hydrogeology Journal, 5, 71–88.

Said, R. (1962) The Geology of Egypt. El Sevier Publ.

Salem, Z. E. S., & Osman, O. M. (2017) Use of major ions to evaluate the hydrogeochemistry of groundwater influenced by reclamation and seawater intrusion, West Nile Delta, Egypt. Environmental Science and Pollution Research, 24, 3675–3704.

Schoeller, H. (1977) Geochemistry of groundwater. Groundwater Studies, an International Guide for Research and Practice, UNESCO, Paris, 1–18.

Sehim, A. A. (1986) Surface and subsurface geologic investigation of Abu Roash area, Western Desert, Egypt. [M. Sc. Thesis]. Cairo University.

Sharaky, A. M., Atta, S. A., El Hassanein, A. S., & Khallaf, K. M. A. (2007) Hydrogeochemistry of groundwater in the Western Nile Delta aquifers, Egypt. 2nd International Conference on the Geology of Tethys, 19(21), 1–23.

Shata, A., & El Fayoumi, I. F. (1967) Geomorphological and morphopedological aspects of the region west of the Nile Delta with special reference to Wadi El Natrun area. Bull Inst Desert d'Egypte, 13(1), 1–38.

Sonkamble, S., Sahya, A., Mondal, N. C., & Harikumar, P. (2012) Appraisal and evolution of hydrochemical processes from proximity basalt and granite areas of Deccan Volcanic Province (DVP) in India. Journal of Hydrology, 438, 181–193.

Srinivasamoorthy, K., Chidambaram, S., Prasanna, M. V, Vasanthavihar, M., Peter, J., & Anandhan, P. (2008) Identification of major sources controlling groundwater chemistry from a hard rock terrain—a case study from Mettur taluk, Salem district, Tamil Nadu, India. Journal of Earth System Science, 117, 49–58.

Sroor, A., El-Bahi, S. M., Abdel-Halieem, A. S., & Abdel-Sabour, M. F. (1999) Organic waste composts, A serious rare-earth source as determined by neutron activation analysis. Nucl. Sci. J. 35 (6), 441–446.

Subramani, T., Rajmohan, N., & Elango, L. (2010) Groundwater geochemistry and identification of hydrogeochemical processes in a hard rock region, Southern India. Environmental Monitoring and Assessment, 162, 123–137.

Sun, Y., Liang, X., Xiao, C., Wang, G., & Meng, F. (2019) Hydrogeochemical Characteristics of Fluoride in the Groundwater of Shuangliao City, China. E3S Web of Conferences, 98. https://doi.org/10.1051/e3sconf/20199809028

Toumi, N., Hussein, B. H. M., Rafrafi, S., & El Kassas, N. (2015) Groundwater quality and hydrochemical properties of Al-Ula region, Saudi Arabia. Environmental Monitoring and Assessment, 187, 1–16.

WHO, G. (2011) Guidelines for drinking-water quality. World Health Organization, 216, 303–304.

Zhu, G. F., Li, Z. Z., Su, Y. H., Ma, J. Z., & Zhang, Y. Y. (2007) Hydrogeochemical and isotope evidence of groundwater evolution and recharge in Minqin Basin, Northwest China. Journal of Hydrology, 333(2–4), 239–251. https://doi.org/10.1016/j.jhydrol.2006.08.013

تقييم متكامل لكيمياء المياه الجوفية لخزانات المياه الجوفية في شمال محافظة الجيزة، باستخدام التحليل الإحصائي متعدد المتغيرات، والنسب الأيونية، والنمذجة الجيوكيميائية

شيرين علي نصر[١]*، علي عبدالمطلب علي[١]، طاهر محمد حسن[٢]، هند سعيد أبو سالم[١]

[١] قسم الجيولوجيا، كلية العلوم، جامعة القاهرة، مصر

[٢] المعامل المركزية لمراقبة جودة البيئة، المركز القومي لبحوث المياه، القناطر الخيرية، مصر

تعد المياه الجوفية مصدرًا مهمًا للمياه في مصر والتي تم استغلالها بشكل كبير في العقود الأخيرة. وقد أدى ذلك زيادة رقعة المناطق المزروعة في غرب دلتا النيل عبر مشروع الدلتا الجديدة (المنطقة الواقعة إلى الغرب من دلتا النيل القديمة)، مما تسبب في ضغوط إضافية على الموارد المائية. تم جمع أربعة عشر عينة من المياه الجوفية من خزان الحقب الرابع الجوفي شبه المحصور، وثلاثة عشر عينة من طبقة المياه الجوفية الميوسينية (المغرة)، وخمس عينات من خزان الحقب الرابع الجوفي غير المحصور، وعينة واحدة من الخزان الجوفي النوبي العميق وتحليلهم للمعايير المختلفة. تم إجراء تقييم شامل لخزانات المياه الجوفية الأربعة في منطقة الدراسة باستخدام التحليلات الإحصائية، المخططات الثنائية، ومخططات بايبر وجبس، بالإضافة الي إجراء مقارنة زمنية لكيمياء المياه. تشير نتائج التحليل الإحصائي إلى أن كيمياء المياه في هذه الخزانات تتأثر بالأنشطة البشرية (العوامل البشرية) والعمليات التي تحدث بشكل طبيعي (العوامل الجيولوجية). كما تشير هيدروجيوكيمياء المياه الجوفية إلى أن خزان الحقب الرابع الجوفي شبه المحصور وخزان المغرة هما الأفضل استخدامًا للري، بينما ينتمي خزان الحقب الرابع الجوفي غير المحصور إلى نوع المياه كلوريد الصوديوم و تتميز مياه الخزان الجوفي النوبي العميق بشدة الملوحة وفقًا لتصنيف الملوحة. بالإضافة إلى ذلك، يجب توخي الحذر للتخفيف من التأثير المحتمل على جودة المياه من التلوث الناتج من استخدام الأسمدة الزراعية وزيادة سحب المياه الجوفية.